U.S. Department
of Transportation
National Highway
Traffic Safety
Administration

NHTSA

DOT HS 813 094

July 2021

Measuring Steering Column Motion in Frontal Rigid-Barrier Test

DISCLAIMER

This publication is distributed by the U.S. Department of Transportation, National Highway Traffic Safety Administration, in the interest of information exchange. The opinions, findings, and conclusions expressed in this publication are those of the authors and not necessarily those of the Department of Transportation or the National Highway Traffic Safety Administration. The United States Government assumes no liability for its contents or use thereof. If trade or manufacturers' names are mentioned, it is only because they are considered essential to the object of the publication and should not be construed as an endorsement. The United States Government does not endorse products or manufacturers.

NOTE: This report is published in the interest of advancing motor vehicle safety research. While the report may provide results from research or tests using specifically identified motor vehicle models, it is not intended to make conclusions about the safety performance or safety compliance of those motor vehicles, and no such conclusions should be drawn.

Suggested APA Format Citation:

Reichert, R., Kan, C.-D., & Park, C.-K. (2021, July). *Measuring steering column motion in frontal rigid-barrier test* (Report No. DOT HS 813 094). National Highway Traffic Safety Administration.

Technical Report Documentation Page

1. Report No.	2. Government Accession No.	3. Recipient's Catalog No.
DOT HS 813 094		

4. Title and Subtitle	5. Report Date
Measuring Steering Column Motion in Frontal Rigid-Barrier Test	July 2021
	6. Performing Organization Code

7. Authors	8. Performing Organization Report No.
Rudolf Reichert; Cing-Dao Kan; Chung-Kyu Park	

9. Performing Organization Name and Address	10. Work Unit No. (TRAIS)
George Mason University Center for Collision Safety and Analysis 4087 University Drive, Suite 2100 Fairfax, VA 22030	11. Contract or Grant No. DTNH2215D00005 693JJ919R000101

12. Sponsoring Agency Name and Address	13. Type of Report and Period Covered
National Highway Traffic Safety Administration 1200 New Jersey Avenue SE Washington, DC 20590	Final – Technical Report Sept. 2019 – Dec. 2020
	14. Sponsoring Agency Code

15. Supplementary Notes

James Saunders (COR) and Ross Jeffries (CO), NHTSA

The authors would also like to acknowledge that Matthias Winkler from Messring and Gerald Goupil with his team at Calspan significantly contributed to this research.

16. Abstract

Federal Motor Vehicle Safety Standard (FMVSS) No. 204, Steering control rearward displacement," specifies a limit on rearward steering column motion in an unoccupied, 30-mph, full-frontal, rigid-barrier crash test. Modern vehicles demonstrate improved energy absorption and steering column designs compared to vehicles prior to the time when FMVSS No. 204 was first introduced.

NHTSA has defined this research task to (1) develop and validate a test procedure to measure dynamic steering column motion during an occupied, 35-mph FMVSS No. 208 frontal rigid-barrier test; and (2) determine if the performance of the steering column motion in a FMVSS No. 208 type test serve as an indication for steering column motion in a FMVSS No. 204 type test.

The George Mason University team has worked with Messring to develop and evaluate different techniques to measure steering column motion in a FMVSS No. 208 type test. The test procedures were demonstrated against two physical frontal rigid-barrier tests which were conducted in cooperation with Calspan. A method to estimate FMVSS No. 204 steering column motion based on FMVSS No. 208 test results was developed.

Simulation studies were conducted to determine how steering column motion and occupant injury metrics correlate. The effect of "Good," "Borderline," and "Failing" steering column motion relative to FMVSS No. 204 on occupant metrics was determined. The simulation studies showed that "Failing" and "Borderline" steering column motion correlated with failing FMVSS No. 208 due to ATD chest deflections of the 5th percentile female and 50th percentile male dummies that were higher than the specified limits for both ATDs.

17. Key Word	18. Distribution Statement
FMVSS No. 204, steering control rearward displacement, finite element simulation, full-scale testing, measuring techniques	The document is available to the public from the National Technical Information Service, www.ntis.gov.

19. Security Classif. (of this report)	20. Security Classif. (of this page)	21. No. of Pages	22. Price
Unclassified	Unclassified	43	

Form DOT F 1700.7 (8-72) Reproduction of completed page authorized

Table of Contents

Executive Summary

Federal Motor Vehicle Safety Standard (FMVSS) No. 204, Steering control rearward displacement," specifies a limit on rearward steering column (SC) motion in an unoccupied, 30-mph full-frontal rigid-barrier crash test. The standard applies to passenger cars, trucks, buses, and multipurpose passenger vehicles (MPVs) with gross vehicle weight ratings (GVWR) of 4,536 kg or less or an unloaded weight of 2,495 kg or less. Modern vehicles are designed for full overlap as well as offset impact configurations. Their frontal structures demonstrate improved energy absorption compared to vehicles prior to or at the time when FMVSS No. 204 was first introduced. In addition, modern restraint systems and collapsible steering column designs have contributed to reduce steering column intrusion and advance vehicle safety.

In responding to a request for comment regarding rules and other agency actions that are good candidates for repeal, replacement, suspension, or modification, the Association of Global Automakers[1] asked whether FMVSS No. 204 continues to provide safety benefits beyond the safety protection provided by FMVSS No. 208, Occupant crash protection, which specifies performance criteria for the driver anthropomorphic test device (ATD) in a 35-mph full-frontal rigid-barrier test. Although FMVSS No. 204 is a vehicle level test, it measures the movement of the steering column toward the driver in the absence of restraints and occupants, whereas FMVSS No. 208 evaluates the occupant protection performance of the whole vehicle through dummy injury criteria. The motion of the steering column in the FMVSS No. 204 test is different from the FMVSS No. 208 test, due to the interaction with the driver ATD and higher impact velocity in the 35-mph impact.

Consequently, NHTSA has defined this research task to (1) develop and validate a test procedure to measure dynamic steering column motion during a FMVSS No. 208 frontal rigid-barrier test; and (2) determine if the performance of the steering column motion in a FMVSS No. 208 type test can predict steering column motion in a FMVSS No. 204 test.

The George Mason University (GMU) team has worked with Messring GmbH[2] to develop and evaluate various techniques to measure steering column motion in the FMVSS No. 208 test. The test procedures were demonstrated against two physical frontal rigid-barrier tests which were conducted in cooperation with the Calspan[3] crash test facility. A method to estimate FMVSS No. 204 steering motion based on FMVSS No. 208 test results was developed. It was found that the residual post-crash steering column intrusion, i.e., the remaining steering hub intrusion into the occupant compartment after the impact, in a 35-mph FMVSS No. 208 with occupant can be a good initial indicator for the maximum dynamic intrusion observed in an unoccupied 30-mph FMVSS No. 204 impact, especially for "Borderline" and "Failing" steering column motion. "Borderline" and "Failing" with respect to FMVSS No. 204 were defined as residual SC

[1] On January 8, 2020, the Alliance of Automobile Manufacturers (Auto Alliance) and the Association of Global Automakers merged to become the Alliance for Automotive Innovation, headquartered in Washington, DC. Members include motor vehicle manufacturers, original equipment suppliers, technology and other automotive-related companies, and trade associations.

[2] A crash testing technology company headquartered in Munich, Germany.

[3] Headquartered and with crash test facility located in Buffalo, New York.

intrusion in longitudinal vehicle direction between 100 mm and 127 mm and greater than the defined reference value of 127 mm, respectively.

Simulation studies with existing vehicle and ATD finite element (FE) models were used to determine how steering column motion and occupant injury metrics correlate. The effect of "Good," "Borderline," and "Failing" steering column motion relative to FMVSS No. 204 on occupant criteria was determined. The conducted simulation studies showed that "Failing" and "Borderline" steering column motion correlated with failing FMVSS No. 208 due to ATD chest deflections of the 5th percentile female and 50th percentile male dummies that were higher than the specified criteria for the respective ATDs.

Documented research conclusions were based on a limited number of simulations and test results. The conducted research forms the basis for potential future work towards a more definitive answer to the question raised by Global Automakers.

1 Introduction

1.1 Background

In 2018, as part of the regulatory review process, the U. S. Department of Transportation invited the public to provide input on existing rules and other agency actions that are good candidates for repeal, replacement, suspension, or modification.[4] The Association of Global Automakers questioned whether FMVSS No. 204, Steering control rearward displacement, continues to provide safety benefits beyond the safety protection provided by FMVSS No. 208, Occupant crash protection. FMVSS No. 204 specifies a limit on rearward steering column motion in an unoccupied, 30-mph, full-frontal, rigid-barrier crash test.[5] FMVSS No. 208 specifies performance criteria for the driver ATD in a 35-mph full-frontal rigid-barrier test.

FMVSS No. 204 is a vehicle level test that measures the movement of the steering control system towards the driver. FMVSS No. 208 evaluates the occupant front crash protection performance of the whole vehicle through dummy injury criteria. FMVSS No. 204 is performed with test equipment that prevents the use of ATDs and the deployment of air bags. A mechanical fixture between the steering hub and the rear of the vehicle is used to measure SC rearward motion. The installment of the fixture makes it necessary to remove the driver seat and driver air bag. It also prevents the use of a "driver dummy."

The primary goal of FMVSS No. 204 is to evaluate the motion of the SC during the crash, the test replaces vehicle components and occupants such as vehicle restraints and ATDs with three redundant measuring devices that ensure the accurate measurement of SC displacement. These devices are (1) a scratch device; (2) painted bands; and (3) linear potentiometers.

The motion of the steering column differs between the two tests due to the interaction between the driver ATD, the deploying air bag, and the vehicle front end crush in the FMVSS No. 208 test. This interaction is not present in the FMVSS No. 204 crash test because no ATD is present. It can be noted that FMVSS No. 204 has negligible opposing forces preventing SC collapse during the crash while FMVSS No. 208 has the opposing forces from the air bags and ATD to lower SC displacement. Additionally, the FMVSS No. 208 barrier test is performed at 35 mph, rather than 30 mph.

Car manufacturers typically provide information regarding compliance with respect to FMVSS No. 204. NHTSA has not conducted FMVSS No. 204 testing recently but has been monitoring residual deformation of the center of the steering wheel in the New Car Assessment Program (NCAP) frontal barrier tests. Differences with respect to front end crush between the FMVSS No. 204 and No. 208 configurations are mainly caused by the different impact velocities of 30 mph and 35 mph, respectively.

[4] 82 FR 45750.

[5] Docket No. DOT-OST-2017-0069.

Consequently, there is an interest in:

(1) Understanding the effect of "Good," "Borderline," and "Failing" SC motion on ATD metrics;
(2) Determining how SC motion compares between FMVSS No. 204 and FMVSS No. 208 crash tests; and
(3) Developing a method to evaluate dynamic steering column performance in future crash tests.

The GMU team used full-scale test data analysis, finite element simulation studies, and measuring technique analyses and full-scale testing in cooperation with Messring and Calspan to address these needs.

1.2 Purpose

The purpose of this task order was to:

(1) Develop a test procedure for measuring dynamic steering column motion in FMVSS No. 208 test conditions.
(2) Develop a methodology to determine if the performance of the steering system in a FMVSS No. 208 type crash test can indicate the expected performance of the steering control system in a FMVSS No. 204 crash test.

1.3 Objective

The two main objectives of this task order were to:

(1) Develop and validate a technique to measure dynamic steering column motion during a FMVSS No. 208 frontal rigid-barrier test. The test procedures were to be verified with a physical test.
(2) Determine if the performance of the steering column motion in a FMVSS No. 208 type test can predict steering column motion in a FMVSS No. 204 test.

2 Data Analysis

2.1 NCAP Full-Scale Tests

In a previous project, the GMU team analyzed more than 200 NCAP full-scale test results including relevant injury criteria used for ATD evaluation in the FMVSS No. 208 type test. U.S. vehicle manufacturers are required to self-certify compliance with all applicable FMVSS. The number of compliance tests performed by NHTSA to verify FMVSS No. 204 self-certification is limited, therefore limiting the amount of publicly available data for recent model year vehicles.

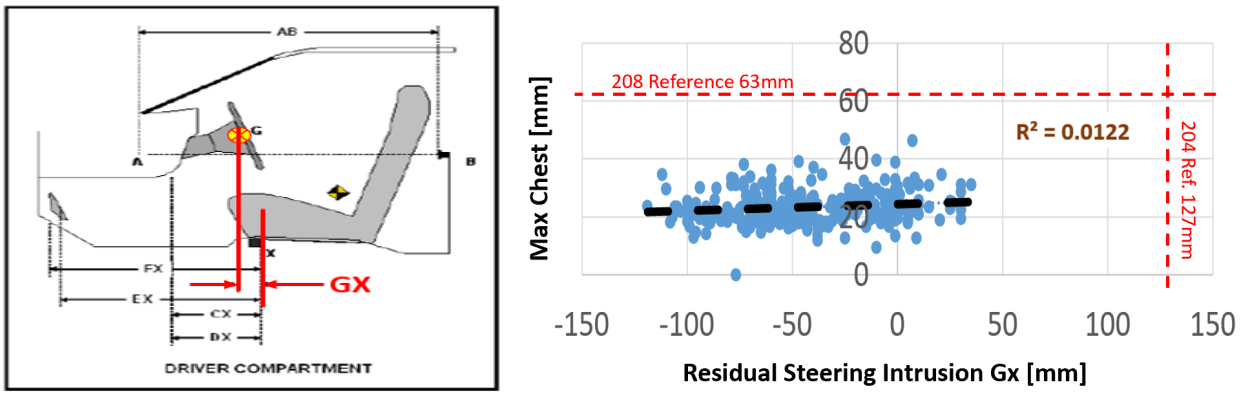

Figure 1. (a) G_x– Residual SC Motion Definition; (b) NCAP Full-Scale Test Data Analysis

The residual SC motion (G_x), as defined in Figure 1 (a), is typically documented in FMVSS No. 208 full-scale test reports. The distance in x-direction between the seat mount and the steering wheel hub, i.e., the center of the steering wheel, is typically measured pre-crash and post-crash. G_x describes the difference between the two measurements. For example, if a distance of 40 mm would be measured before the test and a distance of 70 mm after the full-scale test was conducted, a G_x value of negative (-) 30 mm would be documented, describing that the steering wheel moved 30 mm away from the occupant. Figure 1 (b) shows the correlation between maximum chest deflection and residual SC motion using data from more than 200 full-scale tests. NCAP tests available from NHTSA's vehicle crash test database conducted from 2010 to 2016, representing different vehicle types and models were analyzed. Tests with questionable documented data were removed from the dataset. For all tests, a residual SC motion was documented that was well below the FMVSS No. 204 criteria of 127 mm. For most full-scale tests, a "negative" SC intrusion was recorded, due to SC collapse and displacement due to the interaction with the occupant. The statistical proportion of the variance in maximum chest deflection that is predictable from the residual SC motion, i.e., R^2 was found to be very small. No significant correlation of G_x and chest deflection was observed. However, different vehicle pulses, restraints, and packages significantly affected both injury risk and SC motion.

2.2 NHTSA's Frontal Oblique Full-Scale Tests

In addition to the data analysis conducted for the FMVSS No. 208 type test, more than 100 full-scale crash tests representing NHTSA's frontal oblique impact configuration[6] were similarly analyzed. The dataset consisted of all full-scale research tests available from NHTSA's vehicle crash test database conducted from 2011 to 2016. All vehicles represented the sedan and SUV vehicle classes and different model types, years, and manufacturers. The oblique test condition is not a FMVSS No. 208 test but a research configuration, where an offset moving deformable barrier (OMDB) with a weight of 2,486 kg impacts a stationary vehicle at a speed of 90 kmh. The vehicle is placed at a 15-degree angle from the OMDB longitudinal axis. The impact is set up such that a 35-percent overlap occurs between the OMDB and the front end of the struck vehicle at initial contact, as shown in Figure 2 (a).

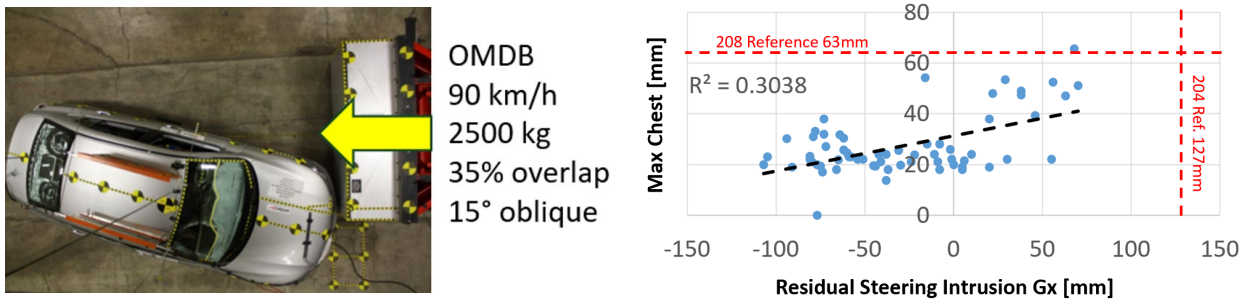

Figure 2. (a) NHTSA's Frontal Oblique Impact Configuration; (b) Oblique Test Data Analysis

Figure 2 (b) shows the correlation between the maximum chest deflection measured using the advanced Test device for Human Occupant Restraint (THOR) dummy and the residual SC intrusion. The measured chest deflection does not describe performance in the FMVSS No. 208 regulation. Few outliers with high chest deflection observed in some of the conducted research tests were included in the analysis. For all tests, a residual SC motion was documented that was well below the FMVSS No. 204 criteria of 127 mm. For most full-scale tests, a "negative" SC intrusion was recorded, i.e., the distance between the seat mount and the steering hub was larger post-crash than pre-crash. A trend of higher chest deflection for higher SC intrusion can be noticed to some extent. There was only one outlier point that exceeded the maximum chest deflection reference of 63 mm, which is relevant for the NCAP full overlap condition but not for the oblique impact research test. The statistical proportion of the variance in maximum chest deflection, i.e., R^2, was found to be small. No significant correlation of Gx and chest deflection was observed. Again, different vehicle pulses, restraints, and packages played dominant roles. It is assumed that these parameters were optimized for the respective vehicles and are responsible for the observed results.

The analyzed modern vehicles demonstrated improved energy absorption and steering column designs compared to vehicles prior to the time when FMVSS No. 204 was first introduced. Tested vehicles complied with FMVSS requirements and were therefor expected to fulfill the FMVSS No. 204 requirement. It was summarized that since none of the FMVSS No. 208 and oblique research tests

[6] National Highway Traffic Safety Administration. (2015, December 5). *Laboratory test procedure for oblique offset moving deformable barrier impact test* (Docket No. NHTSA-2015-0119-0017). www.regulations.gov/document?D=NHTSA-2015-0119-0017.

experienced borderline or failing SC motion per FMVSS No. 204 criteria, simulation studies were found to be better suited to determining the effect of good, borderline, and failing SC motion per FMVSS No. 204 on occupant risk. The results of these studies will be outlined in the next chapter.

3 Simulation Studies

An existing 2015 Toyota Camry FE model was selected to conduct most of the simulation studies. The vehicle had high sales numbers and the simulation model was well validated and exercised in previous research tasks.

FE simulations were used to understand:

(1) The effect of impact speed on occupant responses;
(2) The effect of occupant interaction on steering column motion, i.e., comparison of cases with and without occupants; and
(3) The combined effect of speed and occupant interaction, i.e., 35-mph FMVSS No. 208 condition with occupant interaction versus 30-mph FMVSS No. 204 condition without occupant interaction.

Simulation studies were conducted in accordance with the impact specifications as depicted in Figure 3. FMVSS No. 204 specifies a limit on dynamic rearward steering column motion in an unoccupied, 30-mph full-frontal rigid-barrier crash test, whereas FMVSS No. 208 specifies performance criteria for the 5th percentile female and 50th percentile male ATDs in a 35-mph full-frontal rigid-barrier test. Differences and similarities when using the different ATDs will be outlined in the following chapters.

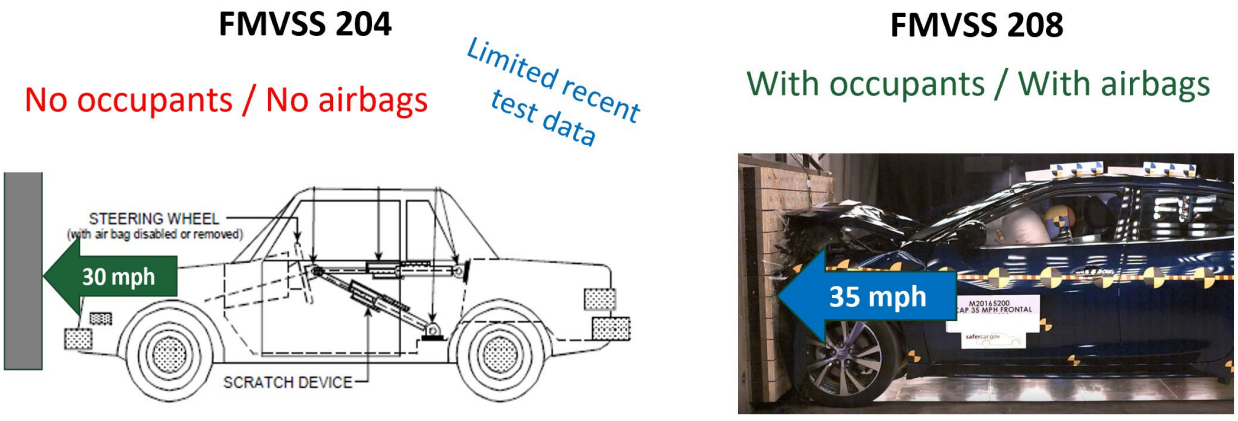

Figure 3. (a) FMVSS No. 204; (b) FMVSS No. 208 – Impact Configurations

The scratch device and mechanical fixture is a tailored mechanical measuring tool, described in the FMVSS No. 204 regulation, that can be equipped with a linear potentiometer to measure the dynamic steering hub rearward motion relative the vehicle in x-direction. Additional details are outlined in Chapter 4.1, Linear and String Potentiometers.

3.1 Simulation Study 1 – Effect of Impact Speed and Occupant Interaction

Figure 4 (a) shows time history data of the steering hub motion from a simulation study that was conducted without occupant at 30 mph, representing the FMVSS No. 204 configuration, and a higher speed of 35 mph. A higher maximum dynamic intrusion was observed for the 35-mph

impact compared to the impact using the 30-mph velocity defined in the regulation. Likewise, higher maximum SC intrusion was observed in the FMVSS No. 208 configuration at 35 mph compared to 30 mph, as shown in Figure 4 (b). Residual SC intrusion and ATD metrics were well below respective reference values in the presented baseline simulation. Similar trends were observed for different vehicle models, i.e., a 2010 Toyota Yaris, a 2014 Honda Accord, and the outlined results from a 2015 Toyota Camry mid-size sedan.

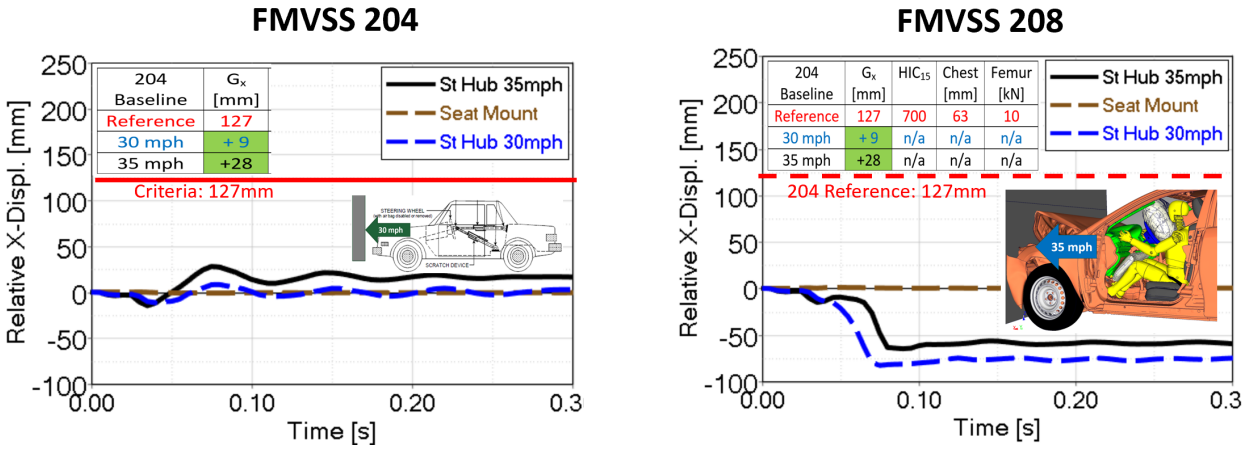

Figure 4. (a) FMVSS 204; (b) FMVSS 208 –- Effect of Impact Speed and Occupant Interaction

3.2 Simulation Study 2 – Effect of Steering Column Motion Using Full Vehicle

A thorough simulation study was conducted to analyze the effect of good, borderline, and failing steering column motion according to FMVSS No. 204 in a full vehicle environment. A maximum dynamic steering column motion relative to the vehicle of less than 100 mm was defined as "Good," a value between 100 mm and 127 mm was defined as "Borderline," and a value greater than 127 mm was defined as "Failing," considering the existing FMVSS No. 204 requirement, which defines a maximum intrusion of 127 mm. The Toyota Camry FE baseline model was compared against available full-scale test data and found to give realistic results with respect to vehicle pulse, steering column motion, and occupant metrics. The model was then modified to produce "Good," "Borderline," and "Failing" SC motion in the FMVSS No. 204 impact configuration and used in the FMVSS No. 208 crash scenario with ATDs in the front driver seat. The FMVSS No. 204 simulations were conducted at a speed of 30 mph without occupant and driver air bag and the FMVSS No. 208 scenarios were simulated with occupant and driver air bag, according to the respective regulations. A direct link between the front of the vehicle and the steering column was implemented to create different amount of SC motion. For example, the linkage point at a more forward location with higher structural deformation was selected for the FE Model that produced "Failing" SC motion. All other parameters such as interior, restraints, SC collapse, and occupant position were kept unchanged compared to the baseline simulation.

Baseline Simulation With "Good" SC Motion

The baseline model was first evaluated without ATD and produced "Good" SC motion in the 30-mph impact, with a maximum relative SC x-displacement of 9 mm, as shown in Figure 5 (a). The baseline simulation model was then used to evaluate the effect on different ATD's, the 50th percentile male and 5th percentile female Hybrid III as shown in Figure 5 (b), and (c). All simulations were conducted at 30 mph and 35 mph and resulting ATD metrics were compared against existing reference values. Realistic values were obtained for all baseline simulations.

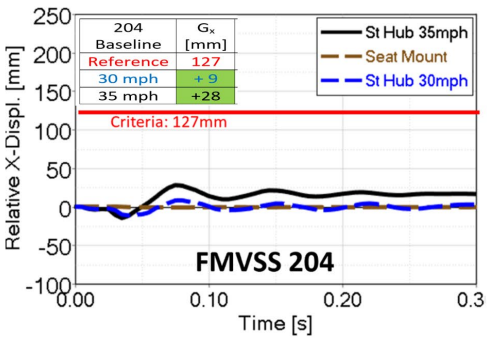

208 Baseline	G_x [mm]	HIC_{15}	Chest [mm]	Femur [kN]
Reference	+127	700	63	10
30 mph	-83	189	29	2.3
35 mph	-65	325	33	2.7

208 Baseline	G_x [mm]	HIC_{15}	Chest [mm]	Femur [kN]
Reference	+127	700	52	6.8
30 mph	-97	95	20	3.3
35 mph	-92	153	27	3.7

Figure 5. (a) 204 "Good" SC Motion; (b) 208 50% Male Hybrid III; (c) 208 5% Female Hybrid III

Simulations With "Borderline" SC Motion

The simulation model that showed "Borderline" SC motion in the FMVSS No. 204 configuration produced a maximum dynamic relative SC x-displacement of 109 mm for the 30-mph impact condition without occupant and restraints, as shown in Figure 6 (a). It can be seen that increasing the speed from 30 to 35 mph causes exceedance of the reference value.

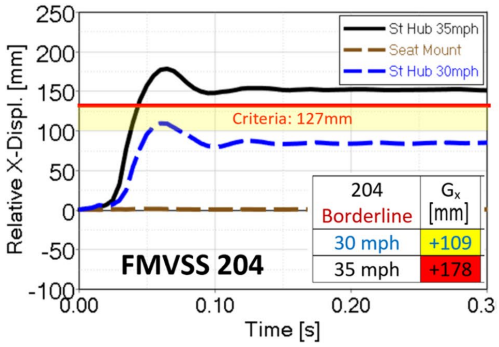

208 Baseline	G_x [mm]	HIC_{15}	Chest [mm]	Femur [kN]
Reference	+127	700	63	10
30 mph	91	246	60	3.8
35 mph	134	549	89	4.5

208 Baseline	G_x [mm]	HIC_{15}	Chest [mm]	Femur [kN]
Reference	+127	700	52	6.8
30 mph	102	570	113	2.8
35 mph	133	803	119	3.0

Figure 6. (a) 204 Borderline SC Motion; (b) 208 50% Male Hybrid III; and (c) 208 5% Female Hybrid III

The model that showed "Borderline" SC motion in the FMVSS No. 204 configuration was then then used to evaluate the effects on different ATD's, the 50th percentile male and 5th percentile female Hybrid III, in the 35-mph FMVSS No. 208 impact configuration, as shown in Figure 6 (b), and (c). It can be noticed that ATD metrics exceeded the used reference values for the chest deflection, when using the vehicle model that showed "Borderline" SC motion in the FMVSS No. 204 configuration. The G_x values for the FMVSS No. 208 configuration shown in Figure 6

(b) and (c) were added for comparison reasons and do not reflect an existing requirement in the 35-mph FMVSS No. 208 standard with a belted occupant. It can also be seen that even though chest deflection exceeded respective reference values, HIC and femur values did not exceed respective criteria.

Simulations With "Failing" SC Motion

The simulation model that showed "Failing" SC motion in the FMVSS No. 204 configuration produced a maximum dynamic relative SC x-displacement of 143 mm for the 30-mph impact condition without occupant and restraints, as shown in Figure 7 (a). The model was then used to evaluate the effect on different ATD's, the 5th percentile female and 50th percentile male Hybrid III, as shown in Figure 7 (b), and (c). It can be noticed that the chest deflection exceeded the used reference values.

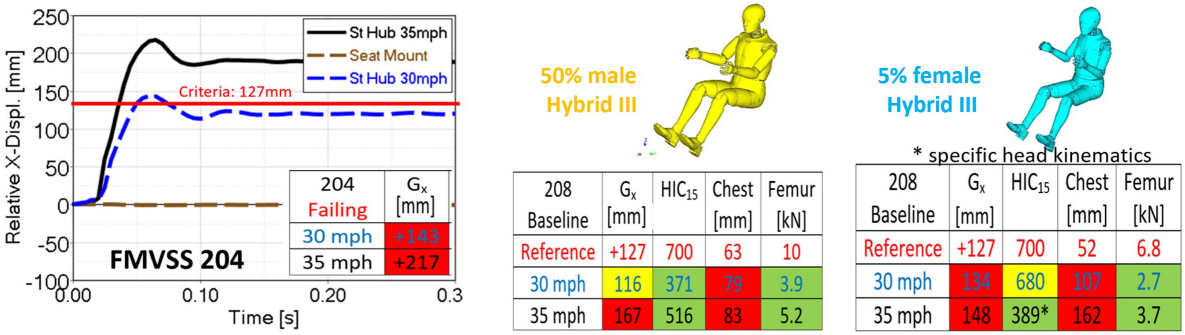

208 Baseline	G_x [mm]	HIC_{15}	Chest [mm]	Femur [kN]
Reference	+127	700	63	10
30 mph	116	371	79	3.9
35 mph	167	516	83	5.2

208 Baseline	G_x [mm]	HIC_{15}	Chest [mm]	Femur [kN]
Reference	+127	700	52	6.8
30 mph	134	680	107	2.7
35 mph	148	389*	162	3.7

Figure 7. (a) 204 Failing SC Motion; (b) 208 50% Male Hybrid III; and (c) 208 5% Female Hybrid III

In conclusion, the results from the simulation study 2 indicated that "Borderline" and "Failing" SC motion with respect to FMVSS No. 204 resulted in failing FMVSS No. 208 based on ATD metrics. Figure 8 (a) shows a snapshot of the different SC intrusion levels on the top and the vehicle velocity pulse for the FMVSS No. 208 baseline and failing simulations at the bottom. It demonstrates that the pulses are practically identical and the effect on the ATD metrics in the FMVSS No. 208 configuration can be purely attributed to the different SC motion. Figure 8 (b) visualizes the differences in steering wheel and ATD chest interaction for the respective SC motions and ATD's. "Borderline" and "Failing" SC motion was created by changing the linkage of the SC to the front of the vehicle without significantly changing the vehicle pulse. Vehicle pulses were measured at the center of gravity of the vehicle using an accelerometer.

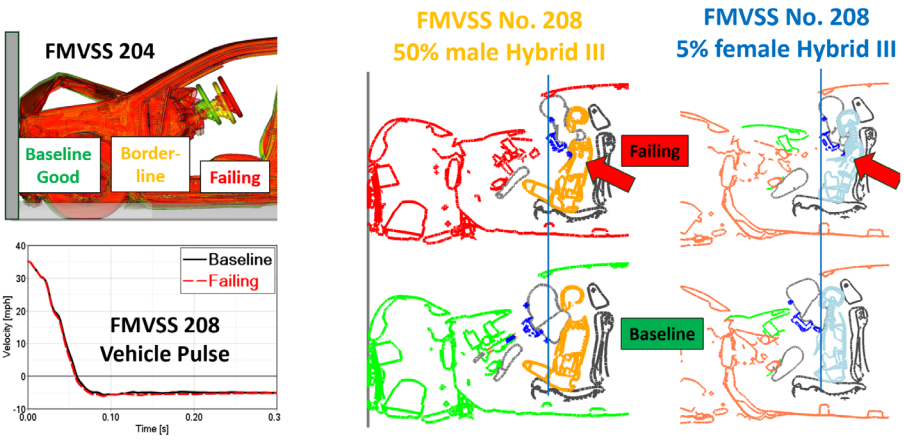

Figure 8. (a) 204 SC Motion and 208 Pulse; (b) "Good" and Failing 208 Cross-Section Views

3.3 Simulation Study 3 – Effect of Steering Column Motion Using Sled Model

A previously developed generic sled model and a representative vehicle pulse were used to analyze the effect of good, borderline, and failing steering column motion with respect to FMVSS No. 204 requirements. More than 200 full-scale NCAP tests were analyzed by the GMU team in a previous study. NCAP tests available from NHTSA's vehicle crash test database conducted from 2010 to 2016, representing different vehicle types and models were selected. An advanced mode analysis method was used to determine representative vehicle pulses, as shown in Figure 9 (a). The mode analysis method included the following steps: (1) data preparation, i.e., data normalization and assembling the entire normalized acceleration vectors into a matrix; (2) Principal Component Analysis (PCA), i.e., use principal components instead of all components to represent the original system; (3) Pules Grouping Process, i.e., each pulse can be represented using a linear combination of a few modes after PCA; (4) Representative pulse generation. A selected representative vehicle crash pulse was applied to the generic sled model. The model included deformable interiors, seat, and restraints, as shown in Figure 9 (b). Variable pulse components (x, y, yaw, pitch) and variable SC motion can be applied to the model. It was developed by the GMU team in cooperation with the Auto Alliance and was previously used to study the effect of reclined and rotated seating conditions in full-frontal, frontal oblique, side, and rear impact conditions.

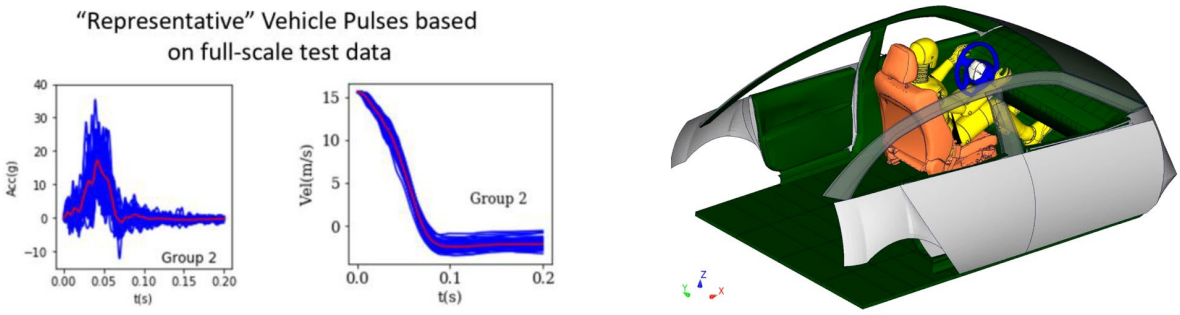

Figure 9. (a) Representative Vehicle Pulse; (b) Generic Sled Model

The existing sled model and representative vehicle pulse produced realistic occupant kinematics and loads for the select boundary conditions, that were based on the FMVSS No. 208 full scale test configuration. Boundary conditions included the initial velocity of 35 mph according to the FMVSS No. 208 regulation and a representative vehicle pulse, describing how the vehicle's velocity changed during the impact, derived from full-scale test data. The resulting occupant kinematics showed the typical forward motion, interaction with the driver air bag and steering wheel, and rebound, known from full-scale testing and full vehicle simulations. A dynamic SC motion, which represented "Good," "Borderline," and "Failing" x-displacement relative to the vehicle was applied, as shown in Figure 10. The dynamic steering hub x-displacement time history data from full vehicle simulation with a "Good" performance was used as a basis. The time history data was then scaled with respect to displacement, to create "Borderline" and "Failing" SC motion. The timing was kept unchanged to account for the realistic qualitative characteristics with a maximum dynamic intrusion at about 70m after impact. This is in agreement with observations from full vehicle simulations and full-scale test data analyses. The modelling approach was found to allow the evaluation the effect of "Borderline" and "Failing" SC motion on ATD metrics. There were no FMVSS No. 208 full-scale crash tests that showed "Borderline" or "Failing" SC motion, and the simulation study approach was found to be an appropriate method to conduct the research study described in Chapter 1, "Purpose" and "Objective."

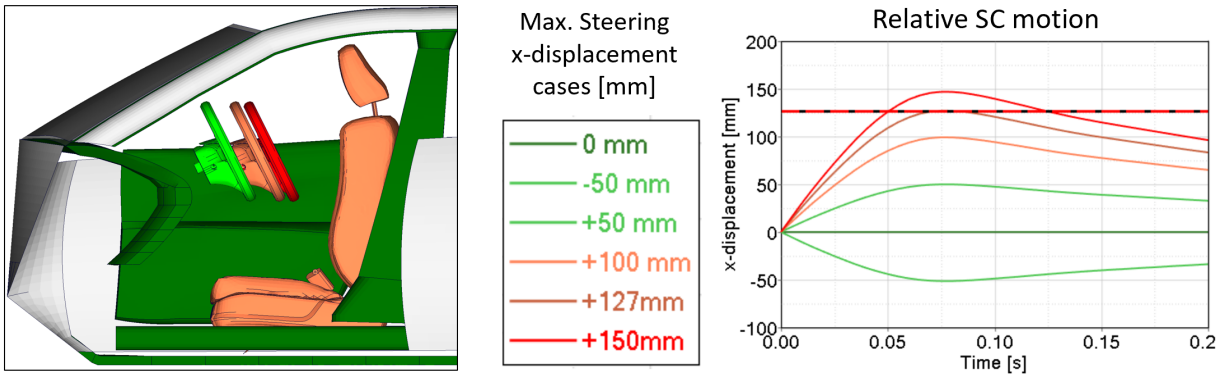

Figure 10. (a) Good, Borderline, and Failing SC Motion; (b) SC Time History Data

A 50th percentile male and 5th percentile female Hybrid III ATD were positioned on the driver seat and used to evaluate the effect of the different SC intrusion characteristics. The simulation that showed a SC motion of negative 50 mm as outlined in Figure 1 and was defined as "Baseline." The SC experienced negative displacement due to occupant contact with the SC in combination with the response of the SC's collapsible design resulting from occupant loading, represented an average value, seen in full-scale tests. SC motion was then increased by 50 mm increments. SC intrusion of negative 50 mm, 0 mm, and positive 50 mm were defined as "Good," SC intrusion of 100 mm and 127 mm were defined as "Borderline," and SC intrusion of 150 mm was defined as "Failing."

"Borderline" and "Failing" SC motion resulted in maximum chest deflection values that were above reference criteria for the mid-size male and small female dummies, as shown in Figure 11.

It can be noticed that for a SC intrusion of 50 mm, which is 100 mm larger than in the baseline simulation, maximum chest deflection for the 5th percentile female ATD exceeded the reference value. This can be explained by the initial position of the 5th percentile female occupant, which is closer to the steering wheel than for the 50th percentile male ATD.

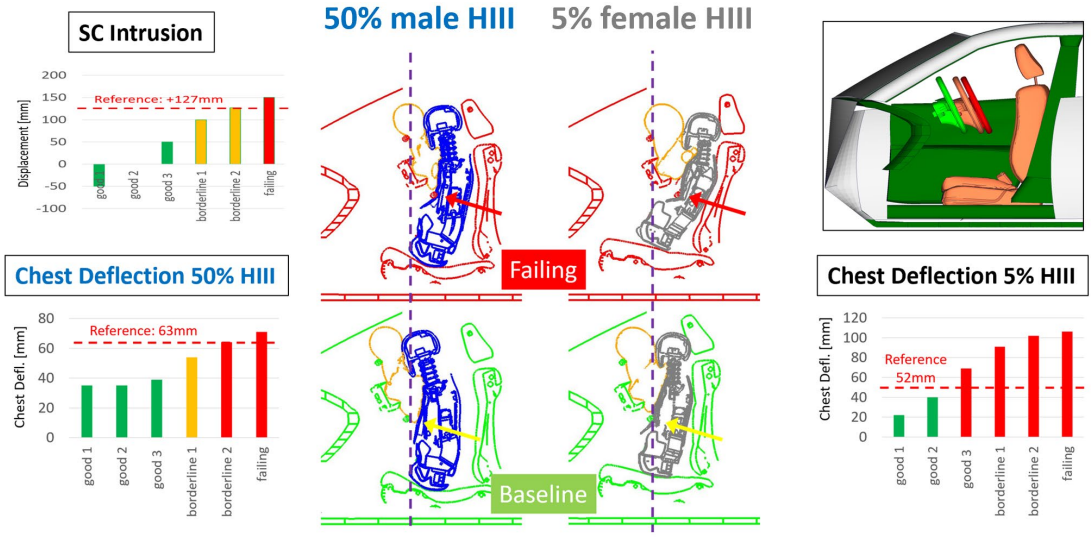

Figure 11. Sled Model Results for 50th Percentile Male and 5th Percentile Female Hybrid III

Figure 12 (a) shows a snapshot of three different SC intrusion levels, i.e., "Good," "Borderline," and "Failing" with respect to FMVSS No. 204. Figure 12 (b) depicts a side view for the FMVSS No. 208 baseline simulation for the 5th percentile female and 50th percentile male ATD's at the bottom and similarly for the simulations with "Failing" SC motion at the top. It visualizes the differences in steering wheel and ATD chest interaction for the respective SC motions and ATD's. The vertical, blue lines highlight the different amount of SC intrusion for the baseline and failing simulations.

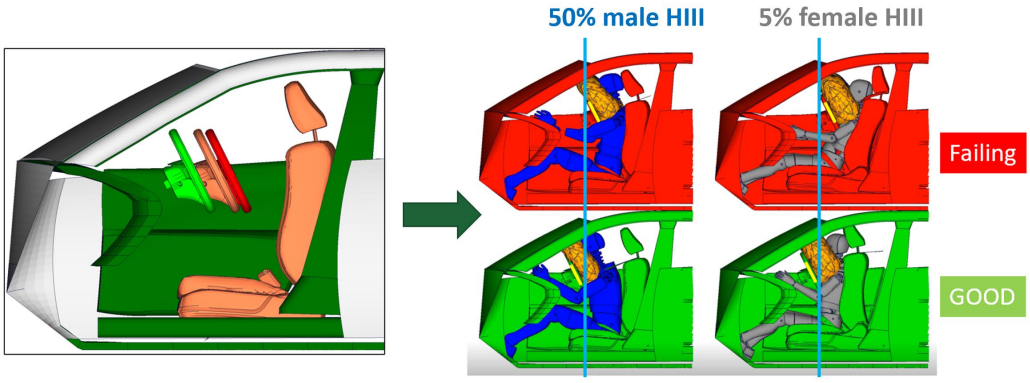

Figure 12. (a) SC Intrusion Levels; (b) 50% Male and 5% Female Hybrid III for "Good" and "Failing" SC Motion

In conclusion, the Simulation Study 3 results using a generic sled model indicated that "Borderline" and "Failing" SC motion with respect to FMVSS No. 204 resulted in failing FMVSS No. 208 results based on 5th percentile female and 50th percentile male ATD metrics.

3.4 Prediction of FMVSS No. 204 SC Motion based on FMVSS No. 208 Results

An existing model of a 2015 Toyota Camry was used to study if the performance of the steering column motion in a FMVSS No. 208 type test can predict steering column motion in a FMVSS No. 204 test. Baseline simulations and full-scale test data were thoroughly studied to determine standard SC motion mechanisms. Three main parameters that typically affect SC intrusion were determined.

These include:

(1) SC collapse;
(2) SC rotation around the mounting point at the Instrument Panel (IP) crossbar; and
(3) potential deformation of the crossbar, as shown in Figure 13.

It was found that some vehicles, i.e., vehicles of different makes and models, experienced SC collapse during a FMVSS No. 208 full-scale test, while others did not. It was evident from the analysis of full-scale tests and simulation data that SC collapse typically occurred when the load from the occupant impacting the steering wheel reached a certain force, usually around 70 milliseconds after the vehicle hit the rigid wall.

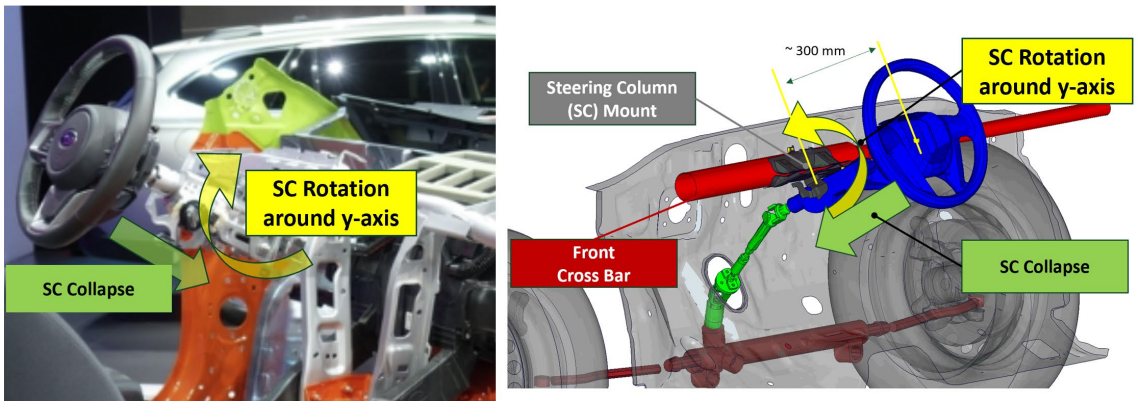

Figure 13. Parameters Affecting SC Motion

SC collapse differs for different vehicle models. As an example, some vehicles have collapsible steering columns that "collapse" when an axial force of about 3,000 newtons is applied. Likewise, significant SC rotation around the mounting point was caused by the interaction with the occupant. Neither SC collapse nor SC rotation was observed in the FMVSS No. 204 configuration due to the absence of the driver.

To verify the described assumptions, simulations with 25, 50, and 75 mm of SC collapse were conducted, as shown in Figure 14.

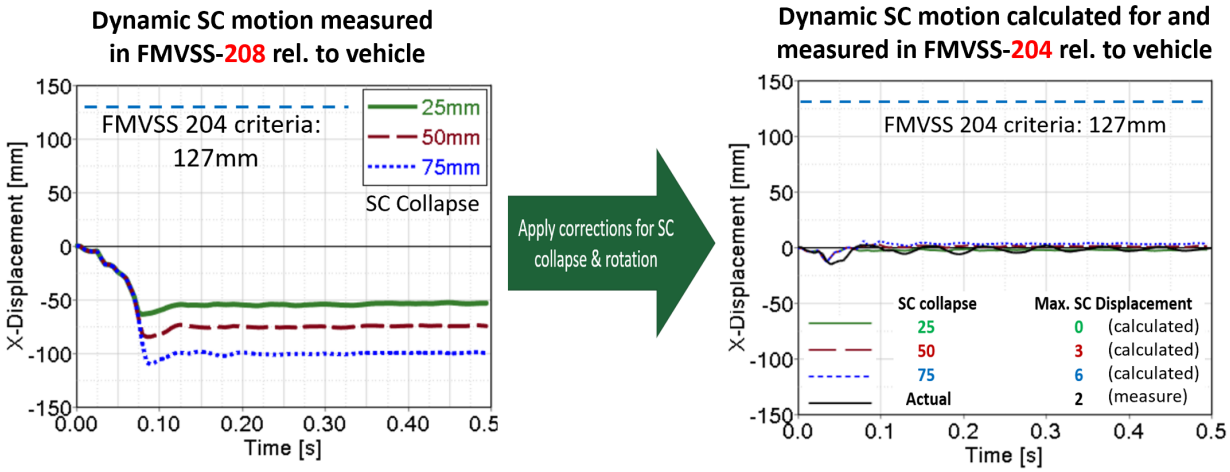

Figure 14. FMVSS No. 204 SC Motion Prediction Based on FMVSS No. 208 Results

Time history data for SC collapse and rotation were recorded. No significant cross bar motion was observed in the baseline simulations. SC x-motion for the FMVSS No. 204 test condition was then calculated for all three FMVSS No 208 cases by subtracting x-motion that was due to SC collapse and rotation. The resulting corrected SC motion calculated from FMVSS No. 208 results was then compared to SC motion from the FMVSS No. 204 simulation. While the actual maximum SC motion was 2 mm, the "predicted" SC x-motion was 0 mm, 3 mm, and 6 mm, respectively. It was concluded that by applying reasonable assumptions, the performance of the steering column motion in a FMVSS No. 208 type test can predict steering column motion in a FMVSS No. 204 test with acceptable accuracy.

The initial simulation study was conducted using the baseline FE model with SC intrusion that is well below the defined limit with respect to the FMVSS No. 204 regulation ("Good"). To verify that the described assumptions would also hold for "Borderline" and "Failing" SC motion, a method was developed to calculate the expected SC motion in a 30-mph FMVSS No. 204 without occupants based on measurements taken during a 35-mph FMVSS No. 208 impact with occupants. The developed formula is outlined below.

Formula to Calculate FMVSS No. 204 SC Motion

Figure 15 depicts a steering column with relevant variables for the calculation of the SC motion in a 30-mph FMVSS No. 204 based on measurements recorded during 35-mph FMVSS No. 208 test.

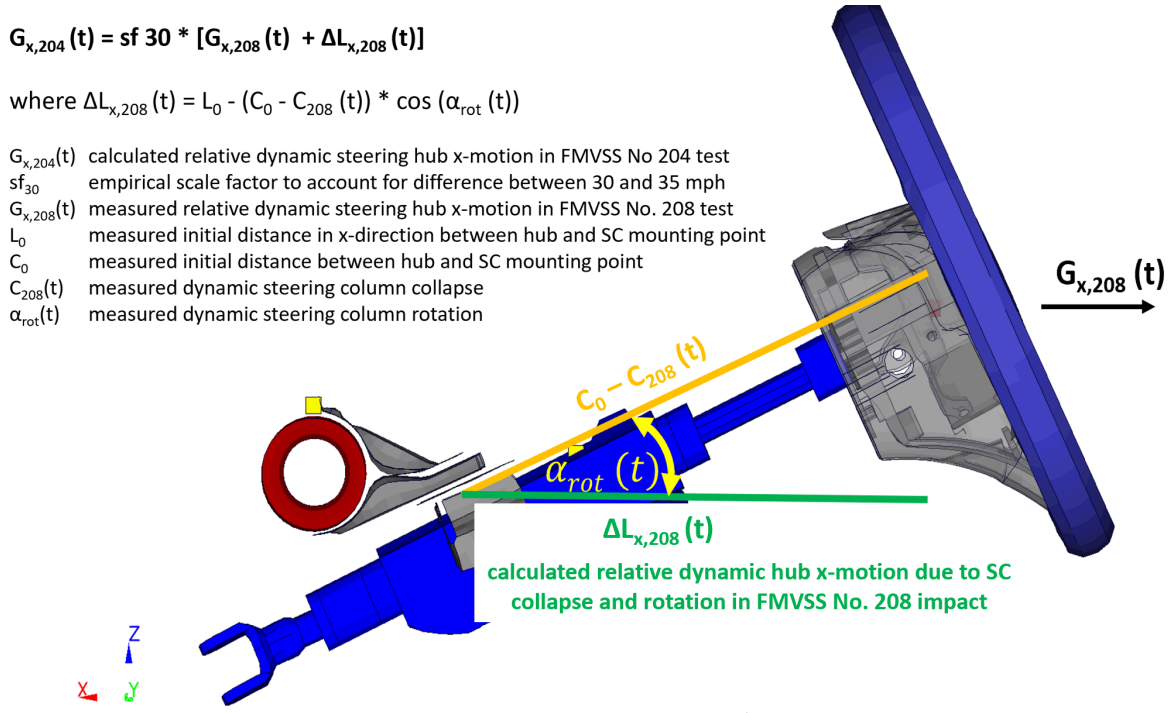

Figure 15. Formula to Calculate FMVSS No. 204 SC Motion

The following assumptions and findings apply:

1) A 35-mph frontal rigid-barrier impact produces higher SC intrusion than a 30-mph impact.
2) SC rotation and SC collapse are mainly caused by the interaction with the occupant.

An empirical scale-factor (sf_{30}) of 0.7 was determined from simulation results to be appropriate to account for the difference in impact speed, especially for "Borderline" and "Failing" SC motion.

Verification and Discussion

Table 1 compares the predicted and actual maximum dynamic FMVSS No. 204 SC intrusions for different cases using the described method. The predicted values were calculated using data from FMVSS No. 208 simulations, as described in the previous paragraph. The actual values represent the maximum dynamic steering column intrusion as recorded from the unoccupied 30-mph FMVSS No. 204 impact.

Table 1: Verification of FMVSS No. 204 SC Intrusion Prediction

SC Motion	Predicted	Actual
Good	3	2
Borderline	123	109
Failing	155	143

It can be noticed that actual and predicted maximum SC intrusion values were of similar magnitude. Predicted values can be judged conservative (from the perspective of which SC intrusion would pass the test) being 10 to 15 mm higher than the actual measurements. This represents a variance of 12 percent and 8 percent for the "Borderline" and "Failing" SC motion scenarios, respectively. The developed method and reasonable assumptions, as described above, indicate the maximum dynamic steering column motion in a FMVSS No. 204 impact based on recorded time history data from the FMVSS No. 208 impact of the same vehicle. Time-history data from the 35-mph impact describing the motion of the steering hub, the SC mounting point, the SC collapse, and the SC rotation were used to calculate the dynamic time history for the steering hub in the 30-mph impact. The dynamic motion of the steering hub in the FMVSS No. 208 configuration can either be directly measured or derived from other measurements, depending on the techniques used. This will be outlined in more detail in Chapter 4. The results shown in Table 1 were taken from a conducted simulation study, where the dynamic motion of the steering hub and any other point relative to the vehicle coordinate system can be recorded. If time-history data from a full-scale test is not available for one or several motion parameters, pre- and post-crash measurements can be used as an alternative and for verification. For example, coordinates of relevant characteristic points at the steering wheel, steering column, and IP cross bar can be measured pre- and post- crash from a FMVSS No. 208 impact to determine deformation, SC collapse, and SC rotation. These can then be used to estimate the FMVSS No. 204 SC motion.

The described method demonstrates that it is possible to use measuring techniques that are currently used in full-scale FMVSS No. 208 type crash test to indicate the expected performance of the steering control system in a FMVSS No. 204 crash test. Additional techniques are described in Chapter 4. Another alternative or complementary practical method is derived from findings from the conducted simulation studies and outlined below.

Table 2 summarizes the residual post-crash and dynamic steering column intrusion for the "Borderline" scenario described Chapter 3.2. Values between 100 mm and 127 mm were defined as "Borderline" with respect to FMVSS No. 204 certification. The recorded maximum dynamic steering column intrusion in the FMVSS No. 204 configuration was 109 mm. It can be noticed that the intrusions were higher for the 35-mph impact compared to the 30-mph impact. It is also evident that the maximum dynamic steering column intrusion is higher than the residual post-crash measurement due to spring-back effects. It can be noticed that the maximum dynamic steering column intrusion in the 30-mph configuration without occupant and the maximum residual post-crash steering column intrusion in the 35-mph impact with occupant showed the same value of 109 mm.

Table 2: Borderline SC Intrusion Summary

	Impact Velocity [mph]	Occupant	Maximum SC Intrusion post-crash [mm]	Maximum SC Intrusion dynamic [mm]
FMVSS-204	30	No	88	109
FMVSS-208	35	Yes	109	134

Table 3 summarizes the maximum residual post-crash and dynamic steering column intrusion for the failing scenario described Chapter 3.2. Maximum dynamic steering column intrusion values above 127 mm were defined as failing with respect to FMVSS No. 204 certification. The maximum dynamic steering column intrusion in the 30-mph configuration without occupant and

the maximum residual post-crash steering column intrusion in the 35-mph impact with occupant showed similar values of 143 mm and 145 mm, respectively.

Table 3: Failing SC Intrusion Summary

	Impact Velocity [mph]	Occupant	Maximum SC Intrusion post-crash [mm]	Maximum SC Intrusion dynamic [mm]
FMVSS-204	30	No	123	143
FMVSS-208	35	Yes	145	173

Similar values for the FMVSS No. 204 dynamic SC intrusion and the FMVSS No. 208 residual SC intrusion can be explained by the following findings:

1) 35-mph impact causes higher intrusion than 30-mph impact.
2) Maximum dynamic intrusion values are higher than residual values due to spring-back effects.
3) SC intrusion is lower when a occupant is present due SC rotation and collapse.

The conducted simulation studies indicated that the described mechanisms, i.e., (1) higher intrusion due to higher impact speed and dynamic measurement on one hand, and (2) lower intrusion due to the presence of an occupant and the resulting SC collapse for the 35-mph FMVSS No. 208 test, balanced each other out. The residual steering hub motion in the FMVSS No. 208 impact can therefore serve as an initial indicator for the maximum dynamic steering hub motion in the FMVSS No. 204 test. The measurement of the residual steering hub motion, represented by the G_x value, is standard in all FMVSS No. 208 full-scale tests. In the event of "Borderline," i.e., G_x values between 100 mm and 127 mm, and "Failing," i.e., G_x values above 127 mm, a more detailed inspection of what caused the high steering column intrusion could be undertaken.

In conclusion, a method to determine steering hub time history data for a FMVSS No. 204 impact based on measurements from a FMVSS No. 208 test was developed. Alternatively, the residual steering hub intrusion, G_x, from the 35-mph impact can be used to indicate performance for the 30-mph impact. In addition, pre- and post-crash measurements around the steering wheel, e.g., at 12, 3, 6, and 9 o'clock, in the future FMVSS No. 208 full-scale tests could be explored further as an indication of FMVSS No. 204 steering wheel motion.

4 Measuring Techniques

The GMU team partnered with Messring to develop and evaluate methods to measure steering column motion and determine its accuracy in a physical FMVSS No. 204 and No. 208 type test. Pre-testing was conducted to determine the capability, repeatability, and accuracy of select measuring techniques. This chapter outlines measuring techniques that were promising and verified in two conducted full-scale tests. Other techniques, such as radio signal, goal line technology, and advanced X-ray techniques were considered but were not found to be promising or practical at this time because of cost and accuracy.

The measuring techniques were used to record time history data of the steering hub in the FMVSS No. 204 and No. 208 type conditions. To obtain extra data from the limited number of full-scale tests, additional measuring locations were defined, as shown in Figure 16. These included a point at the steering rim and a point at the passenger seat's backrest, near the head rest. The additional measuring points experienced more relative displacement and provided additional time-history data to evaluate the various measuring techniques for different motion characteristics.

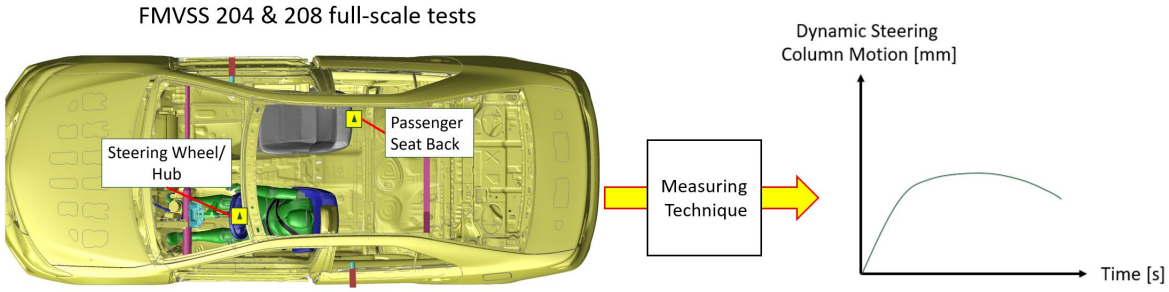

Figure 16. Dynamic Steering Motion Measuring

The following measuring techniques and complementary methods were evaluated.

1. Linear and string potentiometers.
2. Accelerometer and angular rate sensors (ARS) and inertia measuring unit (IMU) sensors.
3. ARS and linear potentiometer at the steering column.
4. Radar sensor.
5. Video tracking.
6. Complementary pre- and post-crash measurements (CMM data).

Specifications, pre-testing results, accuracy, advantages, and disadvantages of the respective methods are outlined in the following sections.

4.1 Technique 1 – Linear and String Potentiometers

The linear and string potentiometers selected to measure steering is Figure 17 (a). A UniMeasure HX-PA Series [7] was used to measure the dynamic steering column motion in the FMVSS No.

[7] See supporting document HX-PA-Linear-Potentiometer-Specifications.pdf (UniMeasure, 2020).

204 type test. Its theoretical accuracy is 0.25 percent or 0.03 inch, which is within the minimum +/- 0.05 inch requirement defined in the regulation. The standard measuring device is known for good repeatability and reproducibility characteristics.

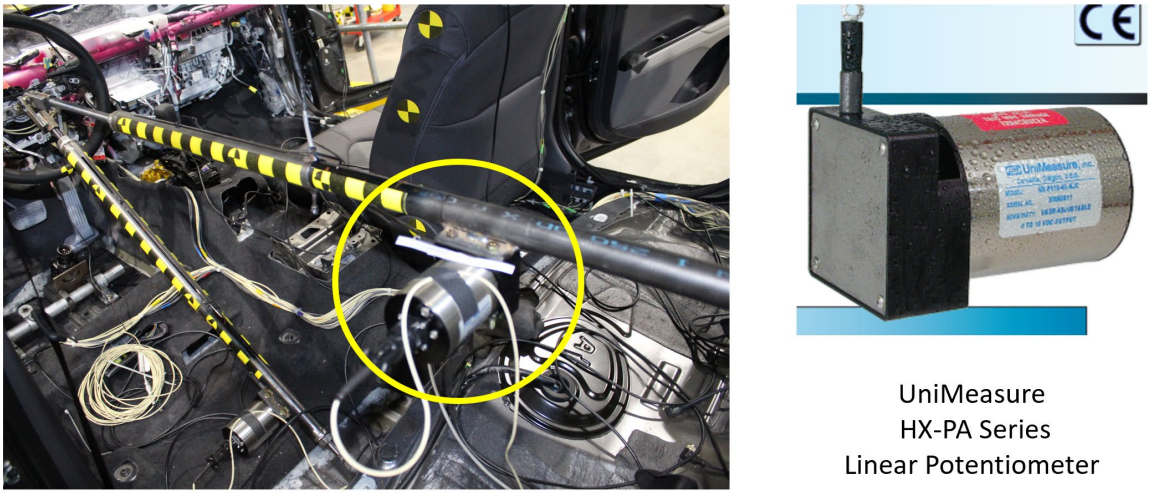

Figure 17. (a) Linear Potentiometer Used for FMVSS No. 204 Steering Hub

The string potentiometers selected to measure steering hub and seatback motion are shown in Figure 17 (b). A LX-PA Series [8] string potentiometer was used to measure steering hub motion in the FMVSS No. 208 test and the passenger seatback motion in the FMVSS No. 204 and No. 208 full-scale tests.

All supporting documents can be downloaded using the link: https://media.ccsa.gmu.edu/s/u7o2dp5m9qw80dq/SC-Supporting-Docs.zip.

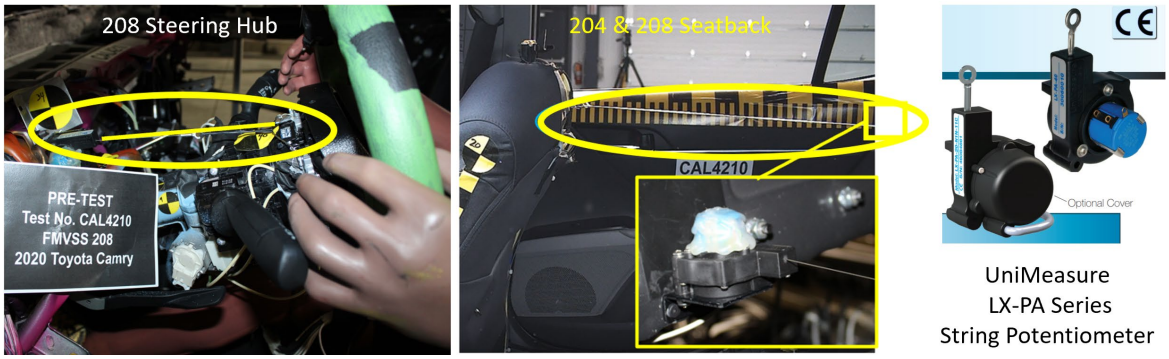

Figure 17. (b) String Potentiometer Used for FMVSS No. 208 Steering Hub and Seatback

[8] See supporting document LX-PA-Linear-Potentiometer-Specifications.pdf (UniMeasure, 2020).

Advantages:

- High accuracy.
- Good repeatability and reproducibility.
- No integration of measured data needed.
- String potentiometers can be easily hooked or attached to points of interest.
- Used products were found sufficient to measure steering hub or seat-back motion.
- Other string potentiometers [9] with higher pull force exist.
- Considered especially reliable for borderline and failing SC motion due to loading direction.

Disadvantages:

- Linear string potentiometer HX-PA in combination with FMVSS No. 204 type fixture, as shown in Figure 17 (a), requires removal of driver seat and air bag and cannot be used for FMVSS No. 208 test with ATD. (In contrast, a string potentiometer mounted forward of the steering wheel, would not interfere with an occupant.)
- String potentiometers with limited pull force can experience "snagging" effects if high motion rates occur in compression direction. This was not observed in the conducted tests.

4.2 Technique 2 – Accelerometers, Angular Rate Sensors, and IMUs

In a previous NHTSA-sponsored research project, a head-tracking tool[10] was developed by the University of Virginia to record ATD head motion relative to the vehicle using accelerometer and angular velocity data. The tool was selected to evaluate if time history data from the SC and rear of the vehicle can be used to determine relative motion. Figure 18 (a) and (b) shows standard accelerometers, ARS, and IMUs[11] mounted to the sill and the passenger seat. The IMUs combine 3 linear acceleration and 3 angular rate sensors. Figure 18 (c) illustrates input variables that are used to calculate the relative motion using the head-tracking tool.

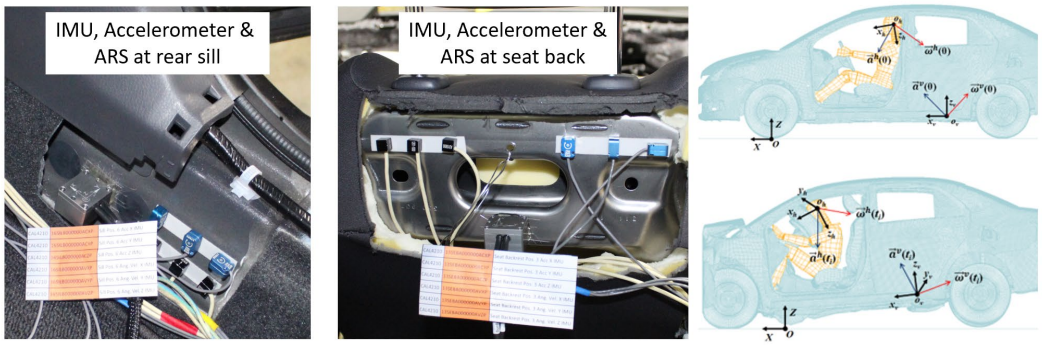

Figure 18. Accelerometer, ARS, IMU's at (a) Sill; (b) Seat; and (c) Calculation of Relative Motion

[9] See supporting document Firstmark-String-Potentiometer-with-higher-pull-force-specifications.pdf (Firstmark, 2020).

[10] See supporting document DHT_software_guidelines.pdf (UVA, 2018).

[11] See supporting document BAY-IMU-specifications.pdf (Bay Sensor Tec, 2020).

Thorough pre-testing has been conducted by Messring for the IMU to evaluate linear acceleration and angular rate characteristics with respect to accuracy, repeatability, and reproducibility. Figure 19 shows a linear sled that was equipped with the IMU's and a radar sensor in addition to a linear gauge measurement scale.

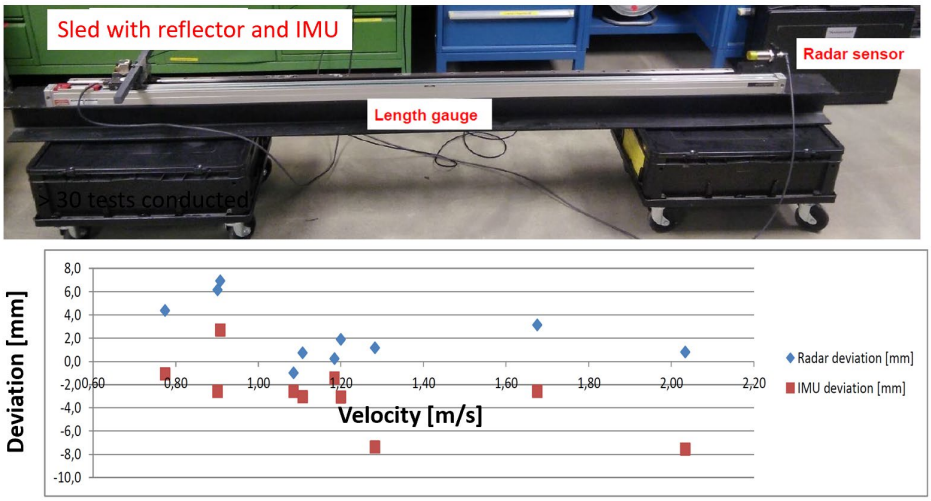

Figure 19. IMU Pre-testing – Linear Sled

Comparing measured displacement from the IMU and actual displacement from the linear gauge showed a deviation of less than 5 percent. Several test series were conducted with consistent test repeatability, reproducibility, and measurement deviation.

A tailored plate with pendulum was developed to evaluate the accuracy of the IMU angular rate measurement, as shown in Figure 20. Measured and actual rotation angles were compared, and good accuracy with a deviation of less than 2 percent was observed.

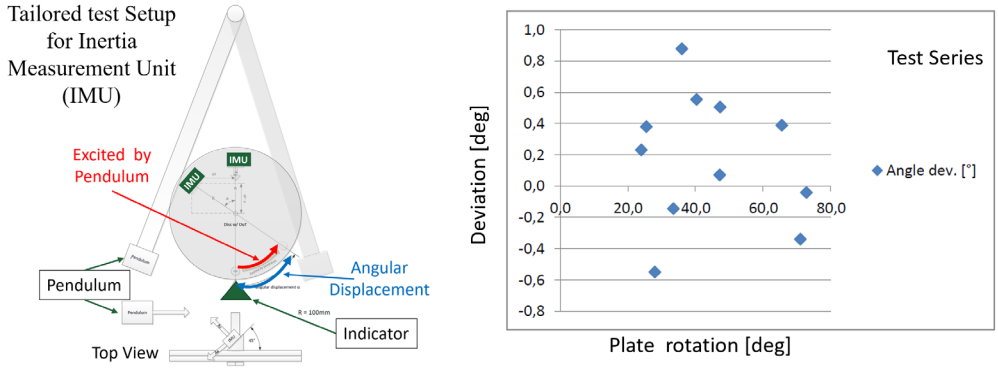

Figure 20. IMU Pre-Testing – Rotation Plate

Advantages:

- Accelerometers and ARS are standard sensors used in crash testing.
- Can be mounted to structural components of interest, such as the sill or SC in a vehicle.
- High theoretical and reasonable experimental accuracy and repeatability on linear sled and rotation plate with well-defined boundary conditions for 1-degree of freedom (DoF) experiments.

Disadvantages:

- Single and double integration are needed to calculate displacement and rotation from measured acceleration and angular rate data.
- High inaccuracy in practical testing was documented due to different factors for 3D tracking as outlined in the final report[12] of the head-tracking tool development. For example, relatively small inaccuracy in measured initial orientation, i.e., 1 degree, may have a substantial effect on the predicted 3D response, i.e., 30mm in x-direction.
- Calculating relative motion such as the steering hub relative to the left sill using the existing head-tracking tool requires a total of 12 reliable time history data channels, i.e., 6 DOF for the steering hub and 6 DOF for the sill. In addition, accurate xyz-coordinate measurements for sixteen points are required to define the exact position and orientation of the data sensors.
- Small inaccuracies in the data for any of the channels or coordinates used to calculate the relative displacement can lead to significant inaccuracies in the final measurement or to questionable results.

4.3 Technique 3 – Linear Potentiometer and ARS

A linear potentiometer, e.g., from the SID2s chest deflection instrumentation, is used by several OEMs to record the dynamic steering column collapse characteristics, as shown in Figure 21. In combination with angular rate measurements around the y-axis, the x-displacement of the steering hub relative to the mounting point can be calculated. The motion of the mounting point and rotation of the SC around the y-axis can be verified using pre- and post-crash measurements. Similarly, motion of the SC due to rotation around the global x- and z-axis, which were found to generally be not significant, can be verified. SC collapse and rotation around the y-axis are typically the dominant components for the dynamic steering column motion in the FMVSS No. 208 full-frontal barrier test.

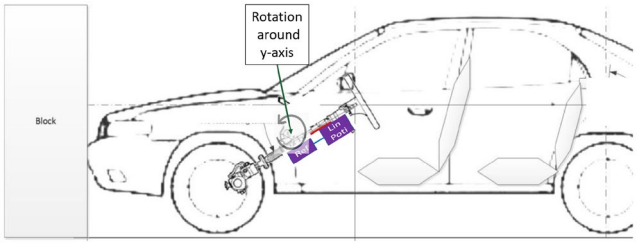

Figure 21. Technique 3: Combined Use of Linear Potentiometer and ARS

[12] Toczyski et. al, "Dummy Head Tracking Software Development," UVA Final Report, 2018.

Advantages:

- Used by OEMs and testing labs during vehicle development.
- Linear potentiometers are accurate, as described in previous section.
- SC rotation calculated from ARS using single integration.
- Relative SC motion can be determined using 2 reliable data channels and verified using pre- and post-crash measurements.
- Standard CMM measurements can be used to verify the measurements; initial SC angle is documented in FMVSS No. 204 and No. 208 tests.
- Standard trigonometrical calculations can be used to calculate the steering hub x-motion from the measured data channels.
- Allows to predict FMVSS No. 204 SC motion from FMVSS No. 208 results using reasonable assumptions.
- No snagging effects were observed during the conducted full-scale tests and "Borderline" and "Failing" steering column motion with respect to FMVSS No. 204 would load the devices in tension and therefore further minimize potential snagging effects.

Disadvantages:

- Requires temporary removal of SC cover to mount linear potentiometer.
- Monitoring of SC mounting point, i.e., pre- and post-crash CMM measurements needed.

4.4 Technique 4 – Radar Sensor

In addition to the previously described measuring techniques used in crash testing, an advanced radar sensor[13] technique was evaluated, as shown in Figure 22. Thorough pre-testing was conducted by Messring. Radar sensor and reflectors were used to record steering wheel rim and seatback motion. A detailed error analysis was conducted and documented.[14] Different objects were placed between the radar sensor and the reflector during pre-testing, as outlined in the radar object detection study.[15] The radar sensor records the strongest reflected radio signal at a 500 Hz frequency within a 6-degree cone. While the reflector amplifies the radar signal, it is possible that a recorded signal shows high oscillation, if a massive steel structure, such as the fixture used in the FMVSS No. 204 configuration is within the measuring cone. In such a case, it can occur, that the reflected signal "jumps" from the reflector to the massive fixture mounted to the steering hub, for example.

[13] See supporting documents 11-baumer-radar-sensor-specifications.pdf (Baumer, 2020).

[14] See supporting documents 12-Radar-error-analysis.pdf.

[15] See supporting documents 13-Radar-object-detection-study.pdf.

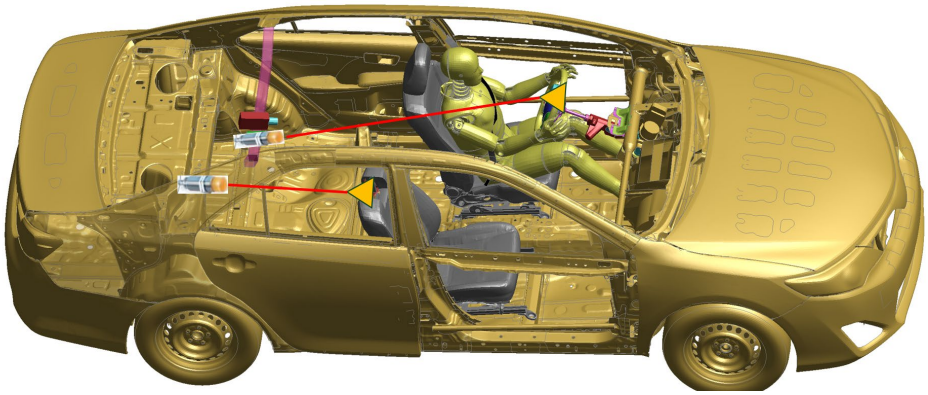

Figure 22. Technique 4: Radar Sensor

Advantages:

- Direct transformation from voltage signal to displacement data.
- No need for data integration.
- Capable to "see through" certain objects, e.g. deploying driver air bag.
- High accuracy in linear sled test.
- Large measurement capacity, i.e., between 0.3 m and 8 m.

Disadvantages:

- Need for thorough calibration and accurate alignment.
- A target with high signal strength, i.e., a reflector, is required.
- Disturbing objects between the sensor and the target can result in signal noise.
- Signal loss from objects that shield the target from the sensor are likely.

4.5 Technique 5 and 6 – Video Tracking and CMM Measurements

Video tracking and CMM data analysis are considered complementary techniques for steering column motion analysis. Video tracking generates time history data for select markers or objects, as shown in Figure 23.

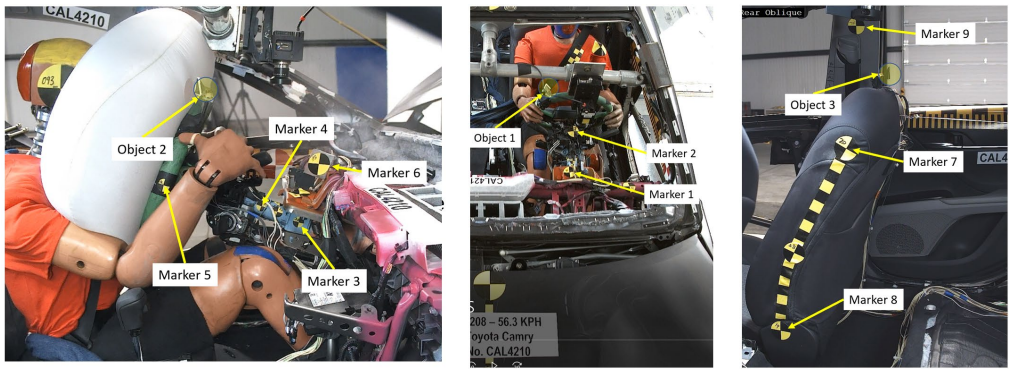

Figure 23. Technique 5: Complementary Video Analysis

CMM data is used to document the location of defined characteristic points, as shown in Figure 24. It can be used as a complementary technique to verify the motion of the mounting point and steering wheel. The residual steering hub intrusion measurement (Gx), which is standard in FMVSS No. 208 testing, is also based on pre- and post-crash measurements of the SC and the seat mount reference point.

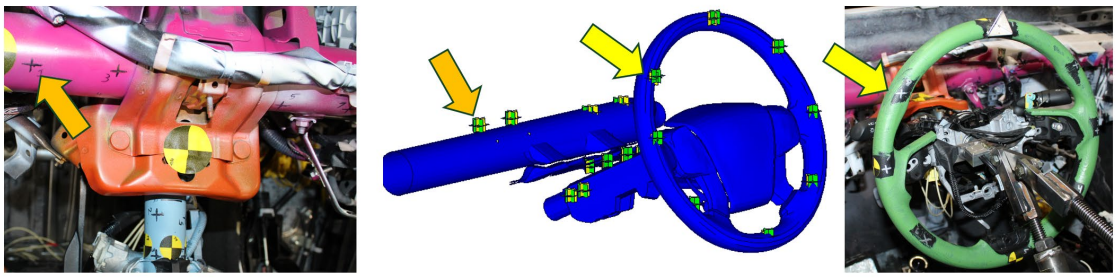

	Pre-Test		
Feature	x	y	z
STEERING WHEEL POINT 1	2,926.16	-344.27	-417.57
STEERING WHEEL POINT 2	2,901.76	-224.25	-357.06
STEERING WHEEL POINT 3	2,863.70	-189.5	-255

	Post-Test		
Feature	x	y	z
STEERING WHEEL POINT 1	2,932.27	-344.585	-414.928
STEERING WHEEL POINT 2	2,907.62	-223.091	-355.472
STEERING WHEEL POINT 3	2,868.73	-188.108	-253.589

Difference		
x	y	z
6.11	-0.31	2.64
5.86	1.16	1.59
5.03	1.39	1.41

Figure 24. Technique 6: Complementary CMM Data

Advantages:

- Standard techniques used by OEMs and test laboratories.
- Can be used as complementary methods to verify other measuring techniques.

Disadvantages:

- Unobstructed view needed for video analysis.
- CMM data only provides information of residual motion, but no time history data.

5 Full-Scale Test Results

Full-scale vehicle crash tests in each of the FMVSS No. 204 and No. 208 test conditions to measure steering column and passenger seatback motion were conducted to verify the selected measuring techniques. The tests were conducted in cooperation with Calspan with a vehicle that fulfilled previously defined selection criteria. The 2020 Toyota Camry was selected because it is high sales numbers in the United States and showed a significant amount of steering column and seatback motion in a previous full-scale test (NHTSA #10146) which uses a vehicle representative of the latest model generation, capturing model years 2018 to 2020. The latest 2020 model year (MY) was selected to ensure full-scale tests were conducted using two "identical," new vehicles to evaluate different measuring techniques. It was determined to be acceptable to use an existing MY 2015 Toyota Camry FE model for the simulation study to understand the effect of different SC motion on ATD metrics and MY 2020 Toyota Camry physical vehicles to conduct the full-scale tests and verify the developed measuring techniques.

5.1 Setup and Instrumentation

The 30-mph FMVSS No. 204 and 35-mph FMVSS No. 208 full-scale crash tests were conducted by Calspan. All air bags, except for the driver air bag in the FMVSS No. 208 test were removed or disabled. Non-structural parts of the front doors and instrument panel as well as the front windshield were removed for better visibility, as shown in Figure 25. A 50th percentile male Hybrid III was positioned in the driver seat in the FMVSS No. 208 configuration.

Figure 25. Full-Scale Tests (a) FMVSS No. 204; (b) FMVSS No. 208

The locations of the test vehicle's instrumentation are summarized in Table 4. Both test vehicles were equipped with the described techniques to measure the steering hub and passenger seatback dynamic motion. The fixture with the linear potentiometer, which is described in the FMVSS No. 204 regulation, was only used for the steering hub in the FMVSS No. 204 test. The radar sensors were used to measure the seatback and steering rim motion with radar reflectors mounted to the steering rim to avoid interference with the FMVSS No. 204 fixture.

Table 4: FMVSS No 204 and 208 Vehicle Instrumentation

	204 SC	208 SC	204 & 208 Seat
204 Fixture including Linear Potentiometer (Hub)	✓	x	x
String Potentiometer	x	✓	✓
Linear Potentiometer for SC Collapse	✓	✓	x
Accelerometers, ARS, and IMU's	✓	✓	✓
Radar Sensor	✓	✓	✓
Video Tracking	✓	✓	✓
Complementary CMM Data	✓	✓	✓

5.2 Data, Videos, Pictures, and Test Reports

All defined data channels on the ATD, SC, and passenger seatback for the FMVSS No. 204 and the FMVSS No. 208 full-scale tests were recorded by Calspan. Furthermore, enough vehicle channels to reproduce the kinematics of the vehicle and high-speed digital color videos, pre-and post-test pictures, and CMM measurements were taken for each test. All data, videos, and photos as specified in NHTSA Test Reference Guide have been provided using a Calspan FTP server. Test reports for the 30-mph FMVSS No. 204[16] and 35-mph FMVSS No. 208[17] full-scale crash tests were created by Calspan and provided as supporting documents.

5.3 FMVSS No. 204 – Steering Hub Motion Analysis

Selected results describing the motion of the steering hub in the FMVSS No. 204 full-scale test are discussed in this section. The results from the linear upper potentiometer attached to the steering hub using the tailored fixture, as shown in Figure 26, are represented by the black solid line. The position of a marker located at the 3 o'clock steering rim position was recorded via video tracking and is represented by the blue dashed line. Similar time history characteristics were observed. The steering hub and the left rear sill location were equipped with IMU's, redundant accelerometer's, and ARS's. Questionable results were obtained from the existing head-tracking tool. As an alternative, the relative motion of the steering hub with respect to the left rear sill was calculated using the x-component data channels only. Higher values and drifting characteristics were observed later in the test, represented by the dotted pink line. This was contributed to the double integration and potential small differences in initial alignment.

[16] See supporting document 14-CAL4209-GMU - 2020 Toyota Camry-FMVSS 204 - Report.pdf.

[17] See supporting document 15-CAL4210-GMU-2020 Toyota Camry-FMVSS 208 Frontal – Report.

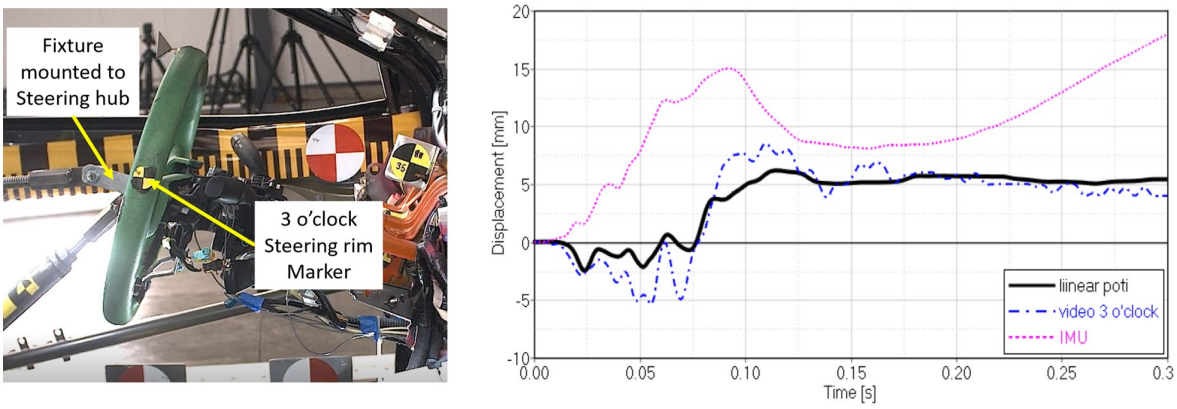

Figure 26. Analysis of Steering Hub Motion (FMVSS No. 204 Test)

In conclusion, the displacement of the steering hub was small as expected. Data from the linear potentiometer and video analysis provided reasonable and comparable results. Processed IMU and tracking tool software were found to provide low quality results and were considered unsuitable for reliably recording accurate steering hub time history data in the full-scale test.

5.4 FMVSS No. 204 – Steering Rim Motion Analysis

The 12 o'clock steering rim position was defined as the second location used to evaluate the previously described measuring techniques, as shown in Figure 27. The radar reflector was mounted at the top of the steering wheel. This added distance prevents the solid metallic tube from interfering with the radar signal that runs parallel to it. Video analysis of footage captured by the onboard camera provides the time history data shown by the solid blue line. It is used as reference for the radar measurement. Higher values were observed for the steering rim than the steering hub. This was expected due to the higher oscillation of the steering rim. The results from the radar sensor, mounted in the rear of the vehicle about 1.8 m from the reflector at the steering rim and aligned in the x-direction, is represented by the red dashed line. Similar overall characteristics with similar maximum values can be observed when comparing the two measuring techniques. The radar signal, processed using a CFC 60Hz filter, showed higher noise than the video analysis signal. It was concluded that the phenomenon where a signal can be reflected by different object, as described in Chapter 3.3, caused the observed oscillations.

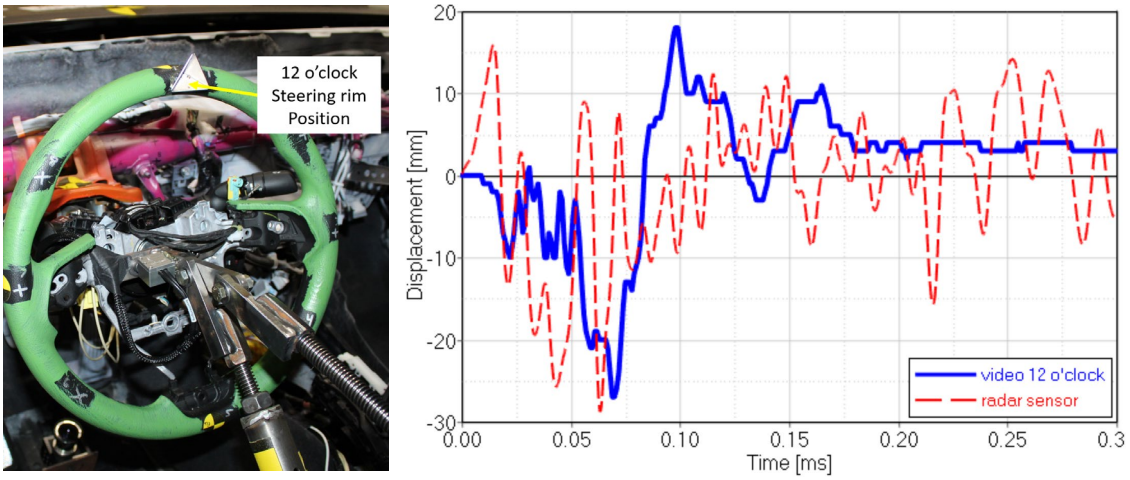

Figure 27. Analysis of Steering Rim Motion (FMVSS No. 204 Test)

In conclusion, a larger amount of motion was observed for the 12 o'clock steering rim location compared to the previously analyzed steering hub position. Similar qualitative characteristics of the signals received from the radar sensor and from the conducted video analysis were found. The video data signal converged to a value that was like the amount of residual displacement, calculated from pre- and post-crash CMM measurements. High oscillation of the radar signal was noted.

5.5 FMVSS No. 204 – Passenger Seatback Motion Analysis

The passenger upper seatback location was used as an additional position to evaluate the previously described measuring techniques. GMU and NHTSA agreed that the position, which was expected to produce potentially higher maximum values than the steering hub, would be appropriate to produce additional output data. Part of the seat foam was removed to be able to access the metallic structure of the seat, as shown in Figure 28 on the left. An existing hole was used to attach one end of a string potentiometer and the other end was hooked to a solid structure in the rear of the vehicle. An IMU was mounted below, and the radar sensor reflector was mounted on top of the string potentiometer measuring location. Markers were placed on the side of the seat at the height of the instrumentations and used for video tracking analysis.

The results from the string potentiometer were defined as reference and are represented by the black solid line in Figure 28 on the right. The seatback first moved forward due to the rigid wall impact and reached its maximum at about 70 ms. It reached the original position after two full oscillation cycles. The video analysis results, represented by the blue dashed line showed similar overall characteristics. Local maxima's after about 100 ms were higher, which can be contributed to small yaw motion of the passenger seat around the z-axis. The radar sensor produced a low noise signal, and its qualitative characteristics were similar to the reference string potentiometer signal. The first peak was lower for the radar sensor which can be attributed to the small distance to the reflector. Similar observations were made during pre-testing with relatively small distances between sensor and reflector.

The relative motion of the seatback with respect to the right rear sill was calculated using the x-component data channels of the installed IMU's, symbolized by the purple dotted line. Higher values and drifting characteristics were observed later in the test which was attributed to the double integration and potential small differences in initial alignment, like the observations made for the steering hub location.

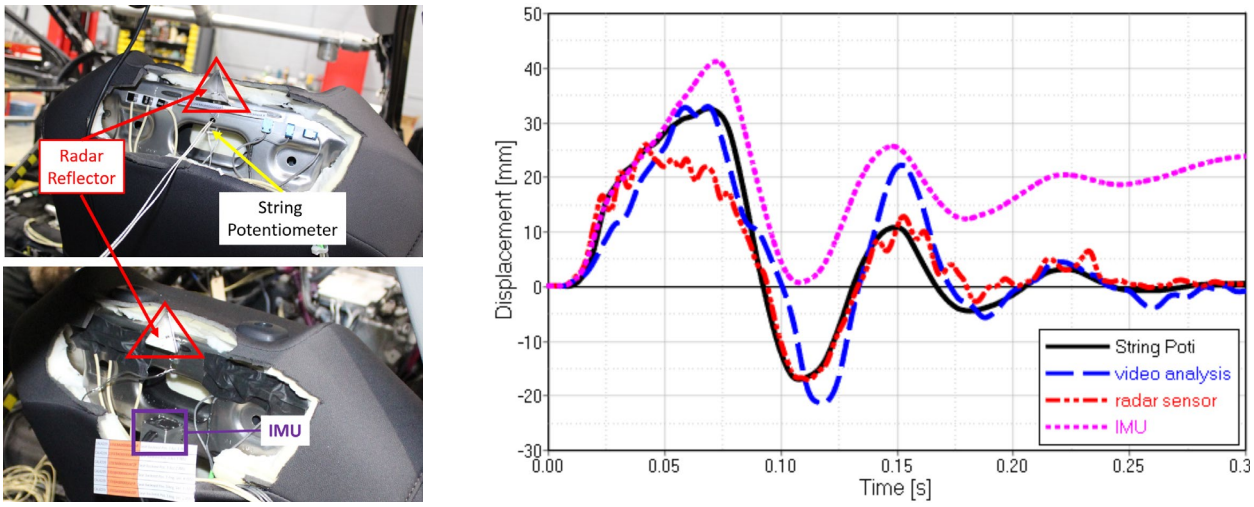

Figure 28. Analysis Passenger Seatback Motion (FMVSS No. 204 Test)

In conclusion, motion of the seatback was higher than for the steering hub, as expected. Data from the string potentiometer and from the video analysis correlated, especially for the maximum value. The radar signal showed lower noise than the signal received from the steering wheel measurement but indicated inaccuracies for maximum forward motion. Data from the IMU's indicated similar qualitative characteristics with inaccuracies for the maximum value and later phase of the motion.

5.6 FMVSS No. 208 – Steering Hub Motion Analysis

The previously conducted FMVSS No. 204 type test determined that the standard string potentiometer produced high quality measurements of the passenger seat's motion. Therefore, a standard string potentiometer was added to measure the steering hub motion in the FMVSS No. 208 type test, as shown in Figure 29 on the left. The simple device can be mounted to structural or interior components made of metallic or thermoplastic material, for example. Ideally the string potentiometer is mounted to measure the motion along the vehicle x-axis. Standard trigonometric functions can be used to correct measurements if the vehicle environment does not allow mounting along the x-axis. Inaccuracies due to measurements from potentiometers that do not perfectly align with the longitudinal vehicle axis are considered to be reasonably small. For example, an angle of 15 degrees between the vehicle x-axis and line of measurement would result in an error of about 3 percent, if not corrected.

A linear potentiometer, also used in the SID-IIs 5th percentile female dummy's chest deflection instrumentation, was attached to the steering column to measure steering column collapse. IMU

and ARS sensors were used to record time history data for the steering hub and the left rear sill. Video analysis as well as pre- and post-crash CMM data was used for data verification.

Select results are outlined in Figure 29 on the right. The motion recorded using the string potentiometer is represented by the black solid line. The peak displacement was higher than in the FMVSS No. 204 configuration and occurred at around 70 ms after contacting the rigid wall due to the interaction with the 50th percentile male Hybrid III, positioned in the driver seat.

The motion of the steering hub along the axis of the steering column is represented by the gray dashed line, recorded using the SID-II 5th percentile female dummy's linear potentiometer. Data from the IMU angular rate sensor was used to calculate the x-motion of the steering hub that could be contributed to the rotation around the vehicle y-axis and the steering column mounting point. By superposing the time-history data measured from the linear potentiometer and the motion due to the steering column rotation, the displacement of the steering hub in vehicle x-direction was calculated. The resulting motion is represented by the green dotted line in Figure 29. It can be noted that the qualitative characteristics and the maximum peak displacement are similar to the data obtained from the string potentiometer which is represented by the black reference curve.

Like for the FMVSS No. 204 type test, questionable data was obtained when using the existing head-tracking tool and displacement was overpredicted when calculating the motion based on acceleration data in x-direction only, represented by the dotted purple line. Video analysis from the onboard camera and data from pre- and post-crash CMM measurements allowed verification of the results.

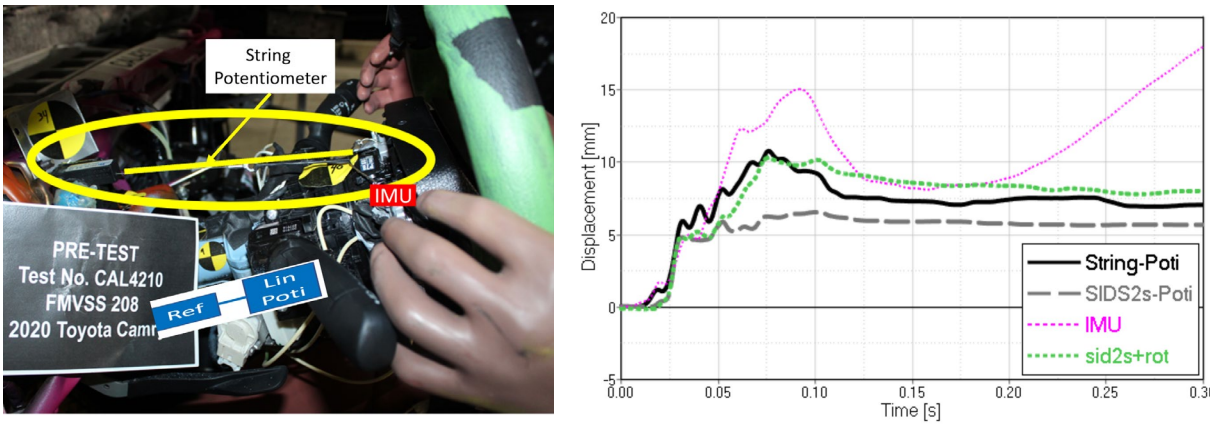

Figure 29. Analysis of Steering Hub Motion (FMVSS No. 208 Test)

In conclusion, reliable time-history data could be obtained using the string potentiometer. Data from a linear potentiometer that measured motion of the steering hub along the steering column axis and from ARS data measuring the rotation of the steering column could be used to calculate the steering hub x-motion. Both time history curves showed similar qualitative characteristics and similar maximum values. Processed IMU and tracking tool software were found to provide

low quality results and were considered unsuitable for reliably determining steering hub time history in the FMVSS No. 208 type full-scale test.

5.7 FMVSS No. 208 – Steering Rim Motion Analysis

The 1:30 o'clock hour hand steering rim position was defined as the second location to evaluate the previously described measuring techniques, as shown in Figure 30 on the left. The main purpose was to determine the ability of the radar sensor to record the time history data in a FMVSS No. 208 type full-scale crash test with an occupant and a deploying driver air bag. The radar reflector was mounted to the steering rim such that it would not interfere with air bag deployment. The radar sensor was located at the rear of the vehicle 1.8 m from the reflector. Figure 30 on the right compares the time history data of the radar sensor, represented by the green dotted line and data from video tracking analysis using the onboard camera mounted to the front passenger door, represented by the solid blue line. It can be noted that both signals have similar qualitative characteristics. A significant displacement in positive x-direction, away from the occupant occurs after about 70 ms due to the interaction of the occupant with the air bag and the steering wheel. The sudden, temporary drop of the radar signal at about 200 ms can be attributed to the occupant's right arm moving between the sensor and the reflector.

A radar sensor signal, with significantly lower noise than observed in the FMVSS No. 204 type test with the massive steering hub measuring fixture, was observed. The driver air bag deployed between the radar sensor and the reflector after about 30 ms and did not obstruct the data signal.

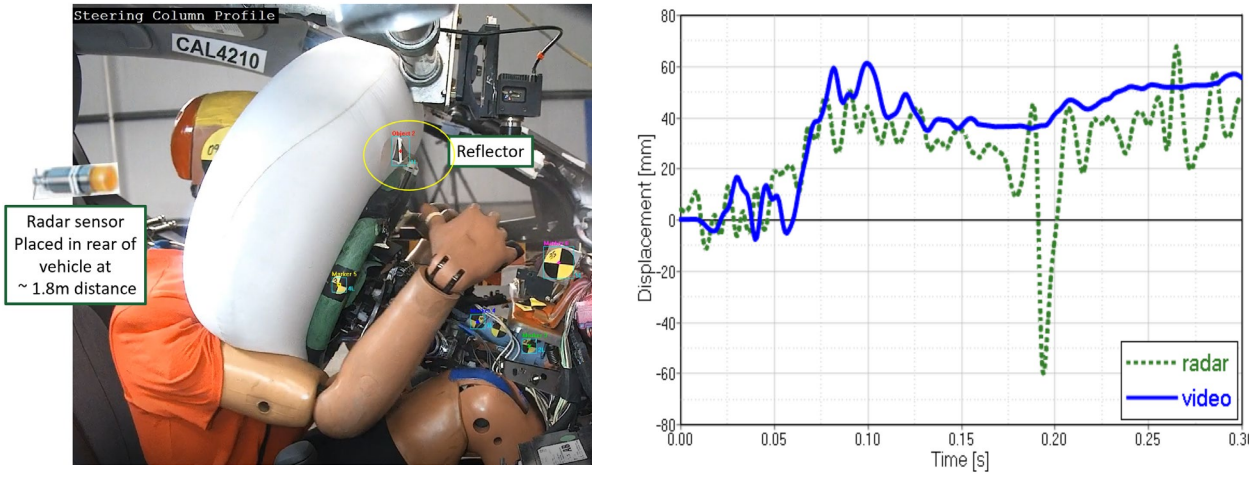

Figure 30. Analysis of Steering Rim Motion (FMVSS No 208 Test)

In conclusion, reasonable data was obtained using the research type radar sensor measuring technique in the FMVSS No. 208 full-scale crash test. It compared reasonably well with the time history data that was obtained using video analysis. The deploying air bag did not disturb the data signal while the occupant's upper arm was temporarily tracked by the radar sensor between 180 and 200ms. The results are considered promising for the new type of measuring technique, but further research would be needed to develop a mature method that can reliably determine steering motion in a full-frontal rigid-barrier crash test with occupants and restraints.

5.8 FMVSS No. 208 – Passenger Seatback Motion Analysis

The passenger upper seatback location was used as an additional position to evaluate the previously described measuring techniques in the FMVSS No. 208 type full-scale test. GMU and NHTSA agreed that the upper seatback position was expected to experience higher maximum values than the steering hub but would be appropriate for recording additional output data. Part of the seat foam was removed to access the metallic structure of the seat, as shown in Figure 31 on the left. One end of a string potentiometer was attached to an existing hole and the other was hooked to a solid structure in the rear of the vehicle, so the potentiometer was aligned to the vehicle's x-axis. An IMU was mounted below, and the radar sensor reflector was mounted on top of the string potentiometer measuring location. Markers on the side of the seat at a similar height as the instrumentation were used for video tracking analysis.

The results from the string potentiometer were defined as reference and are represented by the black solid line in Figure 31 on the right. The seatback moved forward due to the rigid wall impact and reached its maximum at about 70 ms. It reached the original position after three full oscillation cycles. The video analysis results, represented by the blue dashed line, showed similar overall characteristics and maximum forward motion as the string potentiometer. The radar sensor produced a low noise signal and its qualitative characteristics correlated well with the reference string potentiometer signal. The maximum forward motion was lower than what was measured using the string potentiometer and video analysis.

The relative motion of the seatback with respect to the rear sill was calculated using the x-component data channels of the installed IMU's, symbolized by the purple dotted line. Higher values and drifting characteristics were observed later in the test which was attributed to the double integration and potential small differences in initial alignment in agreement with previous observations.

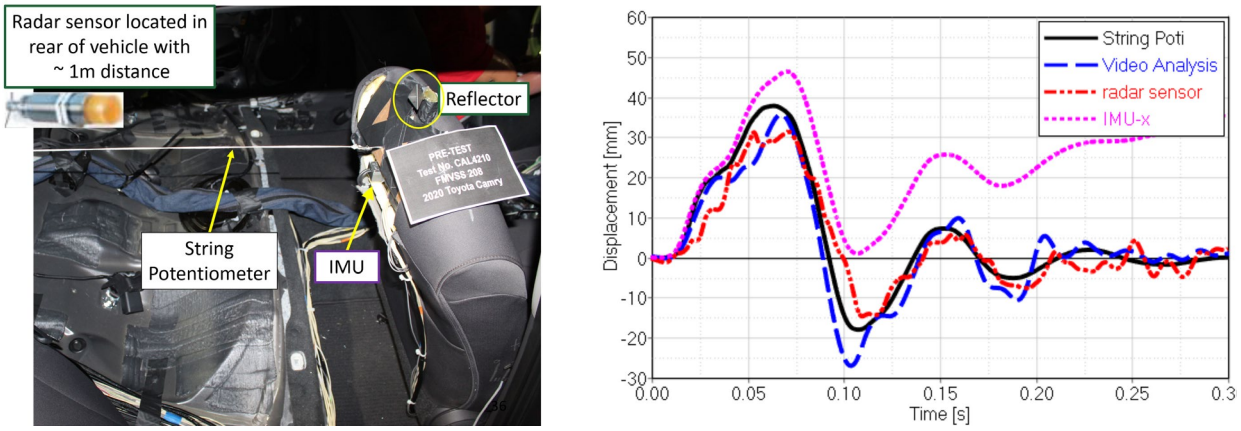

Figure 31. Analysis of Passenger Seatback Motion (FMVSS No. 208 Test)

In conclusion, motion of the seatback was higher than for the steering hub in the FMVSS No. 204 full-scale test for the same measuring location in the FMVSS No. 208 full-scale test. This result was expected due to the higher impact speed. Data from the string potentiometer matched

data from the video analysis especially for the maximum value, reading 38 mm and 36 mm, respectively. The radar signal showed low noise and similar qualitative characteristics as the other measuring techniques. Similar observations were observed with respect to using IMU data as previously described for the other measuring locations.

5.9 Discussion of Capability, Capacity, Accuracy, and Repeatability

The steering wheel and passenger seatback locations were used to evaluate the developed and selected measuring techniques. Data from two full-scale tests was used to evaluate capability, capacity, accuracy, and repeatability of the respective techniques. The results for driver steering wheel and the passenger seatback location complemented theoretical and experimental analyses using linear and pendulum rotational pre-testing for select techniques.

Five different measuring techniques were determined to be promising to allow measurement of dynamic steering column motion in a FMVSS No. 208 full-scale crash test. The techniques include (1) string potentiometers; (2) a combination of linear potentiometer and ARS measurements; (3) radar sensors; (4) IMU data; and (5) complementary video analysis and CMM measurements. Although two full-scale tests do not allow to generate statistically significant data to experimentally determine the accuracy, capacity, capability, and repeatability of the respective methods, clear trends were observed during the full-scale tests. The results were complemented by theoretical and experimental analyses during the pre-testing phase and specifications of the respective measuring techniques.

In summary, all five techniques were found to provide the **capability** to measure steering column and seatback motion with different limitations, as outlined in the previous sections.

The **capacity** of a measuring technique describes the range it can be used for. Different ranges were evaluated during this research. Therefore, it can be concluded that all evaluated methods have the capacity to measure the range of steering motion that can be expected during a FMVSS No. 208 type test.

Conducted pre-testing, full-scale testing, and analyses of theoretical specifications and literature indicated differences in both theoretical and experimental **accuracy** for the respective measuring techniques, as described in Table 5.

Table 5: Accuracy of Measuring Techniques

Theoretical analysis using trigonometrical methods	High
IMU on linear sled (pre-testing)	High
ARS on tailored rotational plate (pre-testing)	High
Measurements based on acceleration and angular velocity measurements from full-scale testing (IMU)	Low (not acceptable)
Radar sensor	Acceptable
Linear and string potentiometers	High
Complementary CMM data	Acceptable

The accuracy of using acceleration and angular velocity data in a full-scale test was found to be not acceptable. This was also outline in UVA's head-tracking tool final report.

A detailed error and accuracy analysis were conducted for radar sensor technology using several linear sled test series and is outlined in supporting document Nr.12. Limitations exist and further research is needed to determine the accuracy of the radar technology in full-scale testing.

Linear and string potentiometers have high theoretical accuracy, as outlined in the respective specifications. Experimental accuracy was also judged sufficient to measure steering and seatback motion. While further research with a statistically significant number of tests would be needed to determine the experimental accuracy for the intended application, potentiometers had the highest experimental accuracy compared to the other techniques evaluated. There is no need for integration of potentiometer data or devices with high pull force.

Reasonable measurement **repeatability and reproducibility** for the respective devices was validated by pre-test and full-scale test results.

6 Conclusion

Existing sedan vehicle and generic sled FE simulation models were used to study the effect of steering column intrusion on ATD metrics. The conducted simulations indicated that "Borderline" and "Failing" steering column motion with respect to the FMVSS No. 204 configuration can result in non-compliance with respect to the FMVSS No. 208 condition due to high chest deflection for both the 5th percentile female and the 50th percentile male ATD in the driver seat.

Conducted simulation studies and analyses of full-scale test data also indicated that significant SC collapse and rotation are mainly caused by the interaction with the occupant in the FMVSS No. 208 test and did not occur in the FMVSS No. 204 configuration. Using these findings, a method was developed to predict dynamic steering column motion in a FMVSS No. 204 test condition from time history data recorded during a FMVSS No. 208 type test.

It was observed that the residual post-crash steering column motion in the 35-mph FMVSS No. 208 test, i.e., the documented G_x value, representing the residual SC motion, can be used as a practical initial indicator for the maximum dynamic steering column motion in the 30-mph FMVSS No. 204 impact. Additional pre- and post-crash measurements around the steering wheel for future NCAP tests would allow to further verify steering column motion and validate the recorded G_x measurement.

Different techniques to measure dynamic steering column motion during a FMVSS No. 208 frontal rigid-barrier test were evaluated and verified. Two methods are recommended based on the conducted research.

(1) The use of string potentiometers was found to be a practical and reliable technique to directly measure steering hub motion.
(2) The use of a linear potentiometer for steering collapse analysis and an angular rate sensor for SC rotation measurement accurately recorded SC motion. Complementary video tracking and coordinate measuring machine (CMM) data measurements can be used to verify the results.

Documented conclusions were based on a limited number of simulation and test results. The conducted research forms the basis for potential future work towards a more definitive answer to the question raised by the Association of Global Automakers.

The conducted research facilitated:

(1) Understanding of the effect of "Good," "Borderline," and "Failing" steering column motion on ATD metrics;
(2) Comparison of steering column motion between FMVSS No. 204 and FMVSS No. 208 crash tests; and
(3) Development of a method to evaluate dynamic steering column performance in future crash tests.

DOT HS 813 094
July 2021

U.S. Department
of Transportation

**National Highway
Traffic Safety
Administration**

15165-070921-v3